Mechanistic Studies of Radical-mediated Polyolefin Modifications

By

Wei Wu

A thesis submitted to the Department of Chemical Engineering

In conformity with the requirements for the degree of

Doctor of Philosophy

Queen's University

Kingston, Ontario, Canada

December, 2008

Abstract

The free radical addition of saturated polymers and small molecules to unsaturated monomers is used to prepare functional derivatives under solvent-free, reactive extrusion conditions. Of particular interest are the dynamics and yields of conventional peroxide-initiated grafting of vinyltrialkoxysilanes to polyethylene, as well as the mechanisms through which bicumene initiates the process at high temperatures. Knowledge of these commercial processes is applied toward the development of new graft modification technology, including radical initiated polymer addition to alkynes, and a new variation of precipitation polymerization chemistry.

The thermolysis of bicumene at temperatures ranging from 220°C to 270°C was used to initiate C-H bond addition from alkanes to vinylsilanes in a high-temperature analogue of conventional grafting practice. The initiation mechanism is shown to involve direct hydrogen atom abstraction by intermediate cumyl radicals, as well as autooxidation processes involving cumyl radicals and available oxygen.

Conventional peroxide initiated graft modifications of polyethylene with vinylsilanes are examined from the standpoint of reaction dynamics and yields. The influence of peroxide loading and monomer concentration on these reaction variables can be described using a simple quasi-steady state kinetic analysis, while the unusual insensitivity of reaction yields to temperature requires further investigation.

A new chemical modification of saturated polymers involving free radical addition to mono-substituted alkynes is presented and examined in terms of reaction yield, graft structure, and changes to molecular weight. Model compounds are used to characterize alkyne grafting products, and to probe the relationship between reagent properties, reaction yields, and product structures.

The discovery of cross-linked particles in the products of polypropylene graft modifications with triallyltrimesate has led to a variation of precipitation polymerization wherein C-H bond addition to an allyl monomer contributes to molecular weight growth, thereby incorporating a significant amount of saturated hydrocarbon into the solid phase. The relationships between reaction conditions and solid-phase composition and morphology are discussed.

Acknowledgements

With a deep sense of gratitude I wish to acknowledge the efforts put forward by my supervisor Dr. J. S. Parent, without whom the completion of this research and thesis could never be possible.

I also want to thank Dr. F. Sauriol and Dr. B. Keller for their assistance with NMR and mass spectroscopy analyses.

I am grateful to Dr. A. Liskova, Dr. S.A.G. Castellanos, Dr. S.S. Sengupta, Ms. A. Penciu, Mr. K.J. Mclean and Mr. M.S. Kaufman for their many and varied contributions to my time at Queen's University.

TABLE OF CONTENTS

LIST OF FIGURES

LIST OF TABLES

LIST OF SCHEMES

Chapter 1 Introduction

1.1 Radical-mediated polyolefin modification.

Polyolefins are a broad class of inexpensive commodity homopolymers and copolymers derived largely from ethylene and propylene, whose chemical stability and mechanical properties are well suited to a wide range of packaging, fluid handling, and non-structural applications. Materials such as polyethylene are easily processed at moderate temperatures using conventional compounding and forming equipment to give low-cost, semi-crystalline products.

Although the saturated aliphatic structure of polyethylene provides good chemical stability, the non-polar nature of this material limits its adhesion to inorganic fillers and polymer blend components. This limits the degree to which fillers can reinforce polyethylene-based composites, and compromises the properties of blends containing polyethylene and materials such as nylon. The softening points of polyolefins also restricts their service temperatures to about 110°C for high density polyethylene and about 140°C for polypropylene homopolymers, above which the article cannot meet most product design specifications.

The commercial potential of polyolefin derivatives that provide good adhesive and/or softening points has fueled interest in chemical modification chemistry. Note, however, that the saturated hydrocarbon structure that underlies the outstanding

physio-chemical properties of polyolefins also makes them difficult substrates for modification. These materials are not amenable to the wide range of ionic and coordination reactions known to organic chemists, and the more forcing reagents they commonly employ cannot be applied in the presence of atmospheric oxygen and moisture. The only practical alternative is free-radical chemistry, which is robust with respect to O_2 and water and can provide the rapid reaction kinetics needed to support short residence time, reactive extrusion processes.

Commercial grades of polyolefin-based adhesives have been created using solvent-free techniques for introducing polar and/or reactive functionality. A leading example is the radical-mediated addition of polyethylene to maleic anhydride, yielding derivatives containing 1-2 wt% of pendant anhydride groups that can hydrogen-bond with siliceous fillers, and react with amine-functionalized polymers such as nylon. [1, 2, 3, 4] Other examples include the grafting of monomers such as vinyl pyrrolidone, acrylic acid, acrylamide to give low-cost materials that, even in small amounts, improve the physical properties of polyolefin composites and blends. [5, 6, 7, 8] The technological applications of graft-modified polyolefin resins are subject of several comprehensive reviews. [9, 10, 11]

Chemical modification techniques have also improved the heat resistance of polyethylene articles by transforming them from thermoplastics into thermosets. These processes involve a shift in polymer architecture from an uncrosslinked state to

one in which every chain is covalently bonded within a continuous polymer network. This restricts chain mobility in the amorphous fraction of the article, thereby improving properties such as stiffness, heat-distortion temperature, abrasion resistance, creep resistance and environmental stress-cracking. The first commercial cross-linked polyolefin was produced by exposing polyethylene to radiation from a Co^{60} isotope. [10] The considerable capital cost of this process led to the development of peroxide-initiated cross-linking, in which radical initiators are incorporated into a polymer melt and activated by thermolysis to give carbon-carbon cross-links.

Polyolefin cross-linking and filler reinforcement technology was advanced considerably by the use of vinyltrialkoxysilane monomers for polyethylene modification. These processes introduce 1-3 wt% of pendant trialkoxysilane groups without grossly affecting the polymer's processing characteristics. These derivatives can be shaped before being moisture-cured through alkoxysilane hydrolysis, allowing goods such as wire coating and tubing to be prepared at high line speeds before rendering them thermoset. Furthermore, polymer-bound alkoxysilane functionality can engage the hydroxyl groups on the surface of siliceous fillers to provide covalent bonds between the polymer and reinforcing agents such as silica and glass fibres. The reviews provide by Al-Malaika and by Plueddemann describe this technology comprehensively. [12, 13]

1.2 Free Radical Graft Modification Chemistry

As noted above, the chemical stability of polyolefins presents a challenge to those interested in producing functional derivatives. The graft modification chemistry applied commercially is a forceful reaction involving the addition of a C-H bond from the polymer across the C=C bond of a suitable monomer. These reactions are remarkable in several respects. Firstly, they create carbon-carbon bonds between polymer and monomer through direct activation of an alkane. Secondly, they are routinely conducted with reaction times on the order of seconds. Thirdly, they introduce a large number of monomer grafts for each molecule of initiator.

These unique qualities are the product of a chain reaction sequence involving highly reactive macro-radical intermediates. A simplified mechanism is provided in Scheme 1.1, where peroxide (ROOR) is used to initiate the addition of a polymer (P-H) to a generic monomer (M).

Scheme 1. 1 Radical initiated polymer grafting process

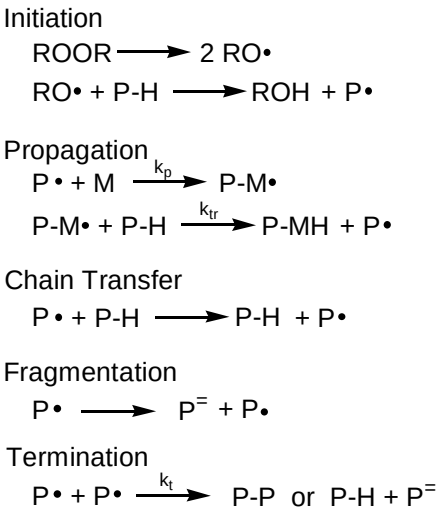

Two comprehensive review articles describe graft modification chemistry in close detail. [14, 15] Moad described each of the reactions illustrated in Scheme 1.1 under polyolefin grafting conditions while discussing the merits of different peroxide initiators, polymers, and monomers that are used commercially and have been studied in academic circles. Russell covered the same topics, with a greater emphasis on reaction dynamics and resulting graft structure. Given these exhaustive reviews, this section of the thesis will examine only those elements of graft modification that pertain to the scope of work. The reader is referred to the aforementioned articles for a broader perspective on the field.

1.2.1 Initiation

The process of adding a C-H bond from a saturated hydrocarbon across a C=C bond of a monomer is initiated by hydrogen atom transfer from the polymer to a peroxide-derived radical. The latter are usually generated by thermolysis in the temperature range of 140°C to 210°C where polyolefins are typically processed by melt extrusion / compounding. In theory, any of diacyl peroxide (1), peroxydicarbonates (2), peresters (3), dialkyl peroxides can be used to initiate graft modification. However, the high decomposition temperatures afforded by alkyl peroxides such as dicumyl peroxide makes them preferable to commercial practitioners of grafting technology.

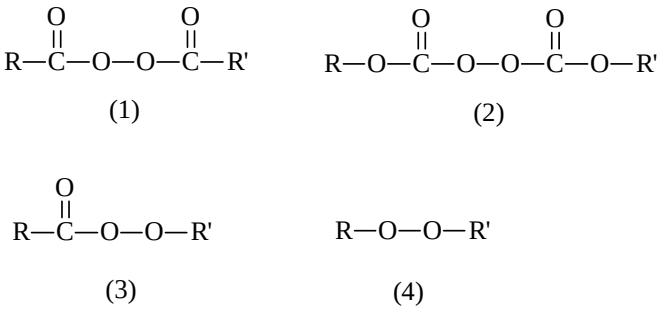

(1) (2) (3) (4)

At the low peroxide concentrations used industrially, the initiator decomposes according to first-order kinetics to give, in the case of dicumyl peroxide, two cumyloxy radicals. These oxygen-centered radical intermediates provide good hydrogen atom abstraction efficiencies from hydrocarbons, [16] preferring hydrogen transfer over addition to electron deficient olefins such as vinyltrialkoxysilanes. This behaviour is distinctly different from the resonance-stabilized, carbon-centered radicals derived from azo-initiators, as well as methyl radicals derived from alkoxy radical fragmentation (Scheme 1.2).[17, 18]

Scheme 1.2 Fragmentation of t-butoxyl.

The multiple pathways through which grafting may be initiated complicates any attempt to understand the process thoroughly. Cumyloxyl and methyl radicals are generated in a 50:50 ratio when dicumyl peroxide is decomposed in dodecane at 140°C, [19] meaning that at least two initiating species must be considered. Furthermore, the potential exists for each of these radicals to add to, and abstract hydrogen from, the monomer added to the system for the purposes of graft

modification. However, the low concentration of vinyltrialkoxysilane used in conventional graft modification reduces the importance of this potential initiation pathway. [19]

1.2.2 Termination

The polymer macro-radicals generated by hydrogen atom donation to initiator fragments are very short-lived, due to rapid termination by radical-radical combination and disproportionation (Scheme 1.3). These elementary reactions follow second order kinetics with respect to radical concentration with rate constants that are limited only by radical diffusion velocities. As a result, rate constants in small molecule media approach 10^9 $M^{-1}s^{-1}$, while their values in polymer melts may be reduced by an order of magnitude. [15]

Combination

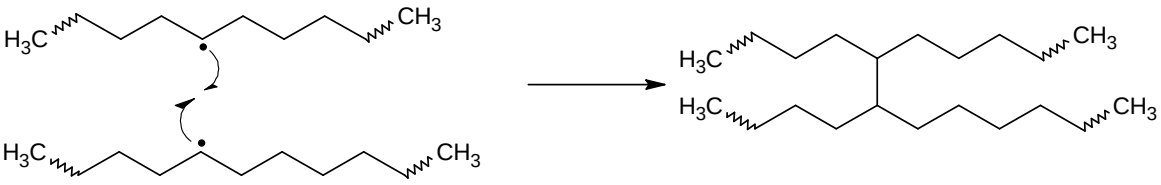

Disproportionation

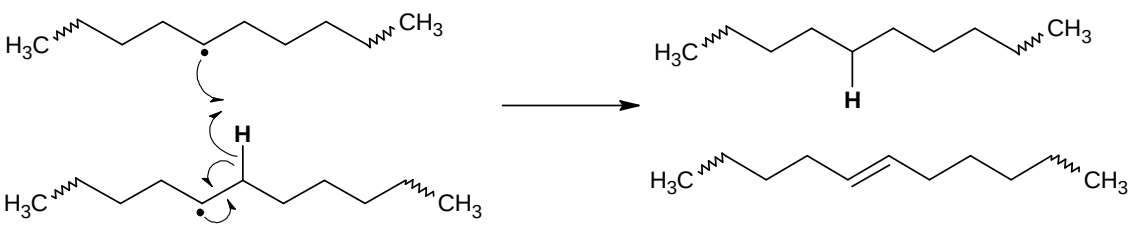

Scheme 1. 3 Combination and disproportionation of polyethylene macro radical.

Termination modes differ greatly between carbon-centred radicals. Representative ratios of the rate constants for disproportionation (k_{td}) and combination (k_{tc}) in aliphatic hydrocarbons at 30°C are k_{td}/k_{tc}=7.2 for *t*-butyl radicals, k_{td}/k_{tc}=1.1 for cyclohexyl species, k_{td}/k_{tc}=0.15 for primary propyl radicals, and $k_{td}/k_{tc}\approx 0$ for allylic radicals. [20] Based on available data, the high temperatures demanded by polyolefin modifications are expected to reduce these ratios slightly. Nevertheless, the tendency for secondary alkyl radicals to disproportionate suggests that polyethylene modifications will undergo a balanced amount of macro-radical combination and disproportionation.

Macro-radical termination does not only affect polymer modification dynamics, it can also affect the product's molecular weight distribution and architecture. Disproportionation has no direct affect on molecular weight, but it introduces undesirable unsaturation to the product which can compromise long-term aging properties. In contrast, macro-radical combination has an immediate impact on molecular weight, as this generates cross-links between polymer chains. This reaction is the basis of polyolefin peroxide cures, but it is generally undesirable for graft-modification processes since cross-linking raises melt viscosity, making the product more difficult to extrude and/or injection mold. As a result, graft modification processes are designed to minimize the amount of peroxide (and the resulting number of macro-radicals) needed to achieve the desired amount of polymer functionalization. This requires careful consideration of graft propagation

efficiencies, as described below.

1.2.3 Propagation.

Two steps are involved in propagation: 1) the addition of polymeric radicals to monomer and 2) the abstraction of hydrogen by the resulting monomer-derived radical (PM·) from a polymer chain. This closed addition/abstraction sequence will proceed until radical-radical termination halts propagation. The ratio of propagation rate versus that of termination is defined as kinetic chain length (KCL, Scheme 1.1).

$$KCL = \frac{k_p[P\cdot]\times[M]}{k_t[R\cdot]^2} = \frac{k_{tr}[PM\cdot]\times[PH]}{k_t[R\cdot]^2} \qquad (1)$$

where [R·] is the total radical concentration. Note that at a given reaction temperature, KCL declines with increasing the radical concentration, which suggests that higher initiator loadings can have a small incremental effect on overall graft yields.

Repeated monomer addition to PM· is always in competition with hydrogen transfer, leading to a possibility of generating oligomeric grafts. Whereas styrene tends to give long chain grafts [26] and maleic anhydride can give pendant dimers when grafted to polyethylene, [27] vinyltrialkoxysilanes give single graft units almost exclusively. [28, 29] Studies of neat vinylsilane polymerizations have reported limited reaction extents when treated with radical initiators, [25] owing to a favourable hydrogen atom abstraction from alkoxy groups. This chain transfer mechanism restricts the degree of polymerization for this monomer, and the dilution of this monomer in excess hydrocarbon suppresses oligomerization entirely.

Note that the hydrogen atom transfer component of graft propagation can proceed intermolecularly or intramolecularly (1, 5-hydrogen abstraction), the latter creating multiple, single-grafts. Whitney et al. [28] studied the radical-initiated vinylsilane grafting to dodecane and found an average of 2.4 grafts per dodecane molecule as single graft units, along with a small amount of oligomerization through chain transfer to ethoxy groups. Parent et al. [29] have similarly reported multiple single grafts of vinyltrimethoxysilane in graft-modified polyethylene.

Alkyl radical fragmentation may accompany graft addition, resulting in the loss of molecular weight. This process has a considerable impact on polypropylene (Scheme 1.4) whose tertiary alkyl radical intermediates cleave significantly at melt temperatures.[14] The β-scission of secondary alkyl radicals is not extensive at temperatures below 180°C, meaning that ethylene rich polyolefins do not lose molecular weight under the action of standard peroxides. [30, 31, 32]

Chain scission:

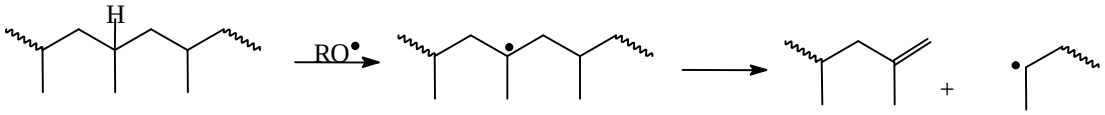

Scheme 1. 4 β-scission of Polypropylene in the presence of radical.

1.3 Thesis Objectives.

This thesis is focused on the free radical addition of polymers and small molecules to

unsaturated monomers to yield functional derivatives under solvent-free, reactive extrusion conditions. The document is divided into four distinct chapters according to subject matter:

1. Dynamics and yields of conventional peroxide-initiated grafting of vinyltrialkoxysilanes to polyethylene,
2. High-temperature vinytrialkoxysilane grafting to polyethylene through bicumene initiation,
3. Polyethylene and poly(ethylene oxide) functionalization by free radical addition to alkyne monomers,
4. Allyl monomer grafting/oligomerization as a variation of precipitation polymerization.

In each case, the objective was to gain insight into the efficiency of the grafting process while understanding how each element of the mechanism contributes to the dynamics and yield of the overall reaction.

1.4 References.

1. Gaylord, N.G.; Ender, H.; Davis, L. and Takahashi, A. *ACS Symposium Series*. **1980**, *121*, 469-475
2. Kim, B.K.; Park, S.Y. and Park, S.J. *European Polymer Journal*, **1991**, *27*, 349-354.
3. Cimmino, S.; Coppala, F.; D'Orazio, L.; Greco, R. Maglio, G.; Malinconico, M.; Mancarella, C.; Martuscelli, E. and Ragosta, G. *Polymer*, **1986**, *27*, 1874-1884.

4. Gaylord, N.J. U.S. Patent 3,645,939, 1972
5. Stanton, G.W. and Traylor, T.G. *U.S. Patent* 3049507, **1962**
6. Iwakura, Y.; Kurosaki, T.; Nagakubo, K.; Takeda, K. and Miura, M. *Bulletin of Chemical Society of Japan*, **1965**, *38(8)*, 1349-1354
7. Sundardi, F. *Journal of Applied Polymer Science*, **1978**, *22*, 3163-3176.
8. Simionescu, C.I.; Macoveanu, M.M. and Cazacu, G., *Acta Polymerica*, **1981**, *32*, 715-718.
9. van Duin, M. *Recent Research Developments in Macromolecules*, **2003**, *7*, 1-28.
10. Munteanu, D. *Reactive Modifiers for Polymers*, Edited by Al-Malaika, S, **1997**, 196-265.
11. Xie, H-Q; Baker, W. E. and Arshady, R., *Desk Reference of Functional Polymers* **1997**, 133-149.
12. Al-Malaika, S. *ACS Symposium Series*, **1988**, *364* (Chem. React. Polym.), 409-425.
13. Pape, P.G. and Plueddemann, E. P. *Journal of Adhesion Science and Technology*, **1991**, *5(10)*, 831-842.
14. Moad, G. *Progress in Polymer Science*, **1999**, *24(1)*, 81-142.
15. Russell, K. E., *Progress in Polymer Science*, **2002**, *27(6)*, 1007-1038.
16. Minisci, F. and Galli, R., *Tetrahedron Letters*, **1962**, *12*, 533-538.
17. Ingold, K.U., *Free Radicals*. **1973,** *Vol. (1)*, J.K. Kochi, ed., Wiley, pg 92.
18. Zytowski, T. and Fischer, H. *Journal of American Chemical Society*, **1997**, *119*, 12869-12878.

19. Parent, J.S., Tripp, M. and Dupont, *Journal of Polymer Engineering and Science*, **2003**, *43*, 234-242.

20. Gibian, M. J. and Corely, R.C. *Chemical Review*, **1973**, *73*, 441-464.

21. Cadogan, J.I.G., *Principles of Free Radical Chemistry*, © The Chemical Society, London, **1973**

22. Mill, T. and Hendry, D.G. *Comprehensive Chemical Kinetics*, **1980**, *16*, 1-87, Ed. Bamford, C.H. and Tipper, C.F.H.

23. Moad,G. *Progress in Polymer Science*, **1999**, *24*, 81-142

24. Russell, K.E. *Progress in Polymer Science*, **2002**, *27*, 1007-1038

25. Mixer, R. Y. and Bailey, D. L., *Journal of Polymer Science*, **1955**, *18(90),* 573-582

26. Kim, B.S. and Kim S. C. *Journal of Applied Polymer Science*, **1998**, *69*, 1307-1317

27. Heinen, W; Rosenmoller, C. H.; Wenzel, C.B.; de Groot, H.J.M.; Lugtenburg, J and van Duin, M. *Macromolecules*, **1996**, *29(1),* 1151-1157

28. Forsyth, J.C.; Baker, W.E. Russell, K.E. and Whitney, R.A., *Journal of Polymer Science, Part A: Polymer Chemistry*, **1997**, *35*, 3517-3525

29. Parent, J.S., Spencer, M. and Whitney R.A. *Polymer*, **2003**, *44*, 2015-2023.

30. Sajkiewicz, P. and Philips, P. J., *Journal of Polyme*r Science*: Part A: Polymer Chemistry*, **1995**, *33*, 853-862.

31. Bremner, T. and Rudin, A., *Polymer Engineering and Science*, **1992**, *32(14),* 939-943.

32. Hulse, G. E.; Kersting, R. J. and Warfel, D. R., *Journal of Polymer Science: Polymer Chemistry Edition*, **1981**, *19*, 655-667.

Chapter 2: Dynamics and Yields of Peroxide-initiated VTEOS Grafting[1]

2.1. Introduction.

Solvent-free reactive extrusion may be the most cost-effective and environmentally-sensitive method of modifying polyolefins modifications[2], but knowledge of the fundamentals of graft-modification has trailed the commercialization of this technology, in part due to the engineering complexities associated with mixing, temperature variations, and residence time distributions that are encountered in compounding extruders [3, 4]. There is also a dearth of information regarding the intrinsic dynamics of grafting chemistry, in that the relationships between grafting rates and reagent concentrations have not been established, nor has the influence of temperature on reaction yields.

VTEOS additions are not only commercially significant, they are also amenable to fundamental study. Unlike maleic anhydride and functional acrylates, VTEOS has virtually no propensity to homopolymerize [5], since hydrogen atom transfer is preferred over repeated monomer addition [6]. Furthermore, VTEOS is soluble in non-polar hydrocarbons and polyolefins, thereby avoiding complications associated with phase-partitioning of monomer and initiator. Recent studies of the structure of VTEOS-grafted hydrocarbons [7, 8] and the dependence of reaction yields on reagent concentrations [9] have provided a basis for a more complete understanding of the dynamics of the grafting process.

Most of the reliable data concerning the structure of graft-modified polymers have been derived from model compounds that can be fractionated and subjected to detailed spectroscopic analyses [7, 10]. Russell and coworkers have extended this approach to study the kinetics of radical-mediated maleation of hydrocarbons [11, 12], and a recent revisitation of this area has led to new insight into the dynamics of this grafting process [13]. While model compound studies benefit from more precise analytical determinations of graft content and more easily controlled reaction conditions, their relationship to solvent-free reactions of macromolecules is unclear. In the present work, we have integrated kinetic studies of model hydrocarbons with yield data derived from linear low density polyethylene (LLDPE) to define the effect of peroxide loading, VTEOS concentration, and temperature on the rates and yields of graft modification.

A further objective of this work was to develop a kinetic scheme of value to practitioners of grafting technology. To be effective in this capacity, a kinetic framework must capture the essential elements of VTEOS grafting without invoking multiple, and often inestimable, rate parameters. The discussion section of this manuscript outlines the principal reactions that support radical-mediated vinylsilane additions that, when taken together, can account for the behaviour of VTEOS additions to hydrocarbons.

2.2 Experimental

Materials. Dicumylperoxide (DCP, 98%), tetradecane (99%) and vinyltriethoxysilane (VTEOS, 98%) were used as received from Sigma-Aldrich. Linear low density polyethylene (LLDPE, octene content = 7.3 mole%, MFI = 1.6 g/10 min) was used as received from DuPont-Dow.

Graft modification of tetradecane. Tetradecane (4.500 g, 22.6 mmole) and VTEOS (0.225 g, 1.18 mmole) were mixed within glass vials fitted with teflon/silicon disks (Reacti-Vials, Pierce) and purged with nitrogen prior to sealing. The resulting solution was stirred within an oil bath for 20 minutes at the reaction temperature prior to injecting the desired amount of DCP in the form of a concentrated solution of peroxide in tetradecane. Samples were withdrawn using syringe at intervals and analyzed for VTEOS conversion by integration of the ^{1}H-NMR resonances of the vinyl group (5.8-6.3 ppm, m, 3H) relative to the resonances originating from the methylene groups of the ethoxy subsitutents (3.8-4.0 ppm, m, 6H). Experiments designed to determine reaction yields were conducted for seven half-lives of the peroxide at the desired reaction temperature.

An estimate of experimental error for reported graft-contents was derived from a series of three independent kinetics experiments, each conducted and analyzed under identical conditions (160°C, [VTEOS] = 5 wt%, [DCP] = 0.05 wt%). A pooled estimate of the variance observed at each reaction time was used to derive a 95%

confidence interval for VTEOS conversion of +/- 0.05, assuming a normal error distribution.

Graft modification of LLDPE. Masterbatches containing the desired amounts of LLDPE, DCP, and VTEOS were prepared at 100°C using a Haake Rheomix 600 internal batch mixer (50 cm^3) controlled by a Haake Rheocord System 40 microprocessor. Purified masterbatches showed no evidence of silane grafting during the mixing procedure and no crosslinking was detected by rheometry over a 20 minute period at the mixing temperature. Melt grafting was accomplished within the cavity of an Alpha Technologies Advanced Polymer Analyzer (3° arc, 1 Hz) at the desired temperature for 6 half-lives of the peroxide, after which the dynamic properties of the sample were recorded at standard conditions (180°C, 3° arc, 1 Hz). Grafted samples (2 g) were purified by dissolving in hot toluene (20ml), precipitating in acetone (100ml) and drying under vacuum (80°C, 0.04 bar). Silane graft contents were determined from FT-IR integrations of the 744-825 cm^{-1} absorbance of silane relative to the 1988-2098 cm^{-1} internal standard region originating from LLDPE. Instrument calibrations were developed using known mixtures of the polymer and octyltriethoxysilane.

Moisture curing and gel content measurement. Grafted polymer (1.0 g) and toluene (20 ml) were heated to reflux and dibutyltin dilaurate (10 μL, 20.2 μmol) was added as catalyst prior the addition of water (0.5 mL). The mixture was maintained at

a reflux condition for 4 hours, after which the polymer was recovered from solution by precipitation with acetone (150 mL) and dried *in vacuo*. Gel content was determined by extracting cured products with refluxing xylenes from 120 mesh sieve cloth. Extraction solutions were stabilized with 100 ppm of 2,6-di-*t*-butyl-4-methylphenol (BHT), and the procedure was conducted for a minimum of 8 hours, with longer times having no effect on the results. The residue material was dried under vacuum to constant weight, and the gel content was calculated as the weight percent of insoluble polymer.

Analysis. FT-IR spectra of thin polymer films were acquired using a Nicolet Avatar 360 instrument at a resolution of 4 cm^{-1}. ^{1}H-NMR spectra were recorded with a Bruker AM-400 spectrometer (400.13 MHz ^{1}H, 100.62 MHz ^{13}C) in $CDCl_3$ with chemical shifts referenced to tetramethylsilane.

2.3 Results

Model Hydrocarbon Graft-modifications.

While it is difficult to control the environment of solvent-free polyolefin modifications, it is a relatively simple matter to regulate the temperature and homogeneity of small molecule reactions. Therefore, we have undertaken a detailed study of dicumylperoxide (DCP) initiated additions of VTEOS to tetradecane, with the latter serving as a reasonable model of polyethylene reactivity. The dynamics of typical grafting processes conducted at 160°C are illustrated in Figure 2.1, in which

VTEOS conversion is plotted against reaction time.

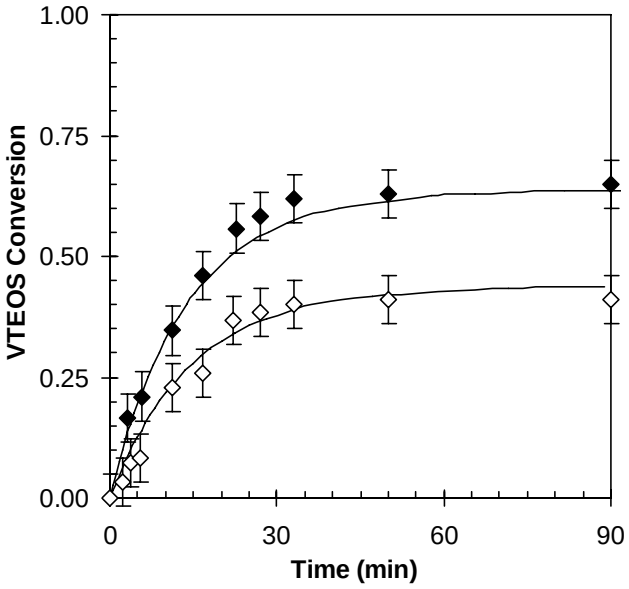

Figure 2.1: Evolution of VTEOS conversion to grafts (tetradecane; [VTEOS] = 5.0 wt%; T = 160°C; ◆: [DCP] = 0.050 wt%; ◇: [DCP] = 0.025 wt%; —— : Equation 10, p33).

As expected, the observed conversion profiles are dominated by the kinetics of peroxide decomposition which, together with radical termination rates, dictate the concentration of macroradicals in the system. The extent to which VTEOS availability affects the grafting rate depends on which element of the graft propagation sequence is rate determining (Scheme 2.1). Unlike conventional monomer polymerizations, an efficient graft-modification cycle involves a closed sequence of radical addition and hydrogen atom transfer. If monomer addition is rate-limiting, the overall grafting rate is expected to abide by first-order kinetics with respect to [VTEOS], whereas if hydrogen abstraction is rate-determining, the rate of graft formation will be independent of the monomer concentration. Given the present state of knowledge regarding the graft propagation sequence, an unambiguous

assignment of a rate-determining step cannot be made with confidence. However, we will show that this assignment is not required to derive a useful kinetic model of the process.

Figure 2.2 demonstrates the dependence of VTEOS conversion to grafts on initiator concentration. Peroxide yields, defined as the moles of VTEOS grafted per mole of cumyloxy radicals generated by DCP homolysis, varied from a low of 22 grafts per radical at a peroxide loading of 0.15 wt%, to a high of 66 when just 0.015 wt% of initiator was employed. These results confirm that the vast majority of monomer is consumed through the graft propagation sequence, and that the chain-carrying radical intermediates are the polymer-derived and monomer-derived radicals (P· and V· respectively) illustrated in Scheme 2.1.

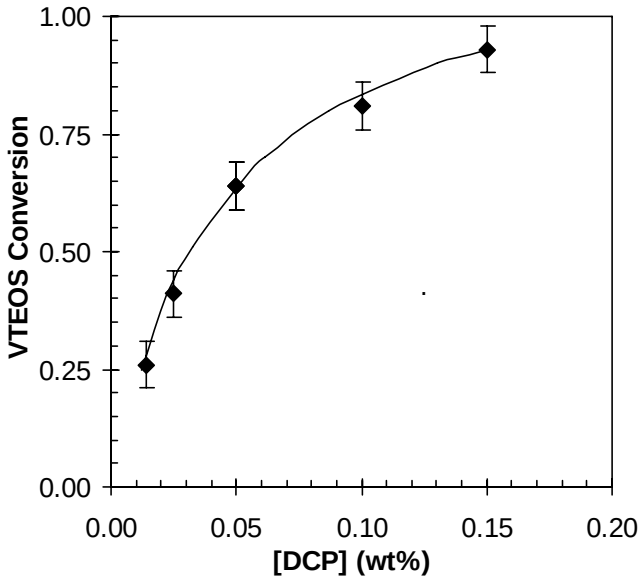

Figure 2.2: Ultimate VTEOS conversion as a function of peroxide loading (tetradecane; [VTEOS] = 5.0 wt%; T = 160°C; ◆: experimental data; —— : Equation 10, p33).

Scheme 2. 1 Detailed DCP initiated Polyolefins grafting onto VTEOS.

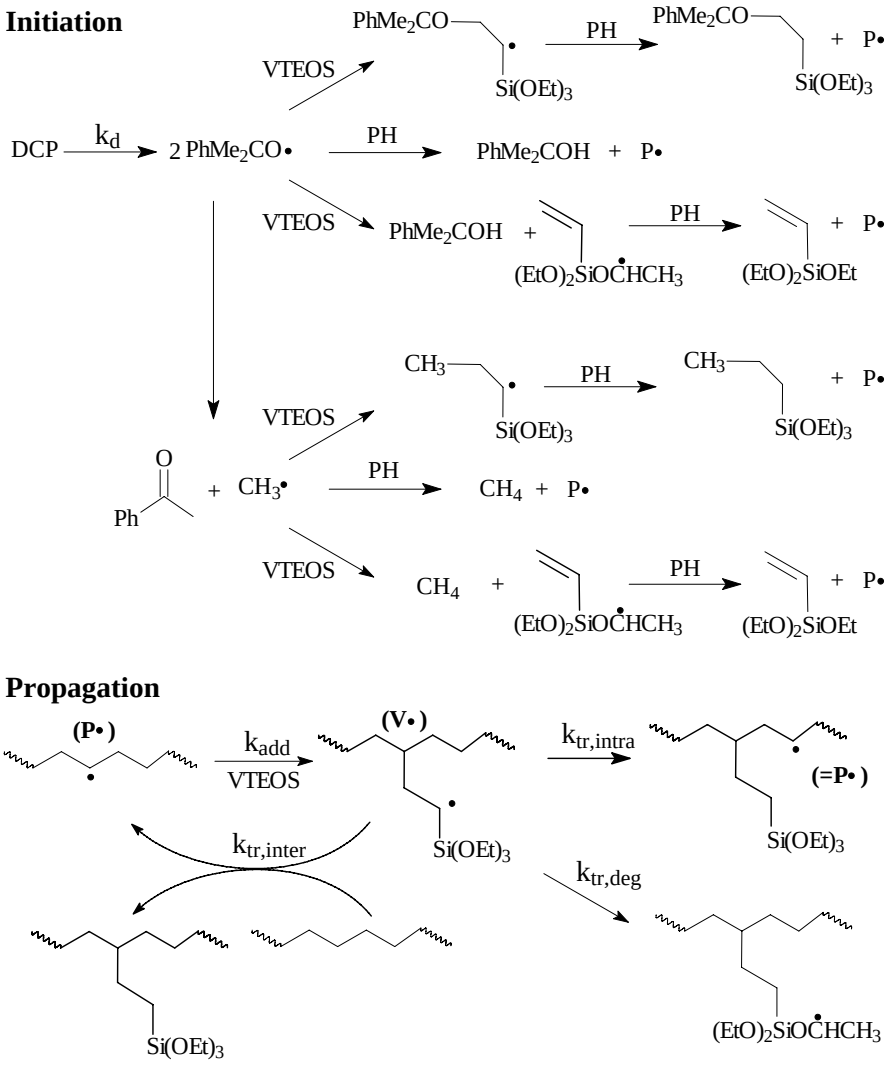

Of particular interest is our observation that ultimate graft yields are insensitive to reaction temperature (Figure 2.3). This behaviour is surprising in that the half-life of DCP declines from 14.97 min to 0.83 min as its decomposition temperature is raised from 150°C to 180°C. Since accelerated initiator decomposition is expected to result in a sharp decline in radical lifetime, higher reaction temperatures are expected to

impact negatively on grafting yields. We will discuss the origin of this unexpected temperature insensitivity following a brief examination of a linear low density polyethylene (LLDPE) system.

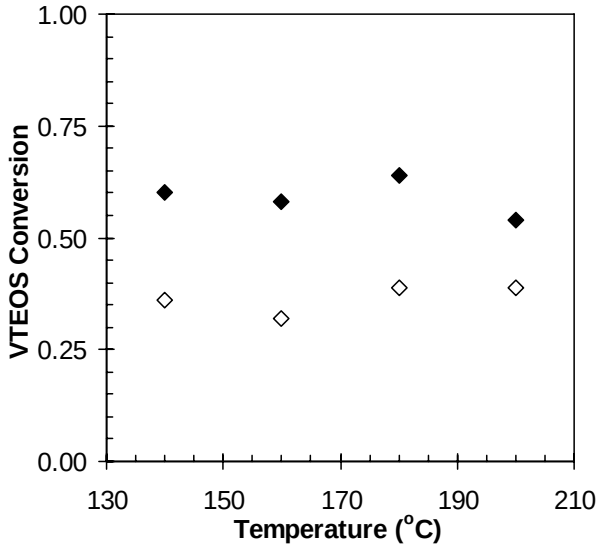

Figure 2.3: Ultimate VTEOS conversion as a function of grafting temperature (tetradecane; [VTEOS] = 5.0`wt%; ◆ [DCP] = 0.05 wt%; ◇ [DCP] = 0.025 wt%).

LLDPE Graft-modifications.

LLDPE modifications were accomplished by reacting premixed masterbatches within the cavity of a controlled-strain oscillatory rheometer. In addition to providing the complex viscosity data needed to assess the extent of polymer crosslinking, the instrument provided exceptional temperature control and a pressurized, melt-sealed environment that prevented monomer volatilization. This methodology provides isothermal, batch reaction data that do not suffer from complications associated with atmospheric oxygen, and non-ideal residence time distributions, the well-mixed samples from masterbatches exclude the possible mixing issues. Therefore, our data pertain to intrinsic grafting chemistry which, when integrated with knowledge of

polymer processing factors, can yield a complete description of a reactive extrusion process.

The conversion of vinylsilane to LLDPE-g-VTEOS grafts is presented as a function of peroxide loading in Figure 2.4. While the response of reaction conversion to DCP loading is consistent with that observed for the model compound (Figure 2.2), peroxide yields recorded for LLDPE ranged from 4.4 to 8.4 grafts per radical. Differences in initiation efficiency, macroradical reactivity, and the inhibitory effects imposed by the antioxidants that are present within commercial polyolefins are contributing factors to the reduced reactivity of the polymer system.

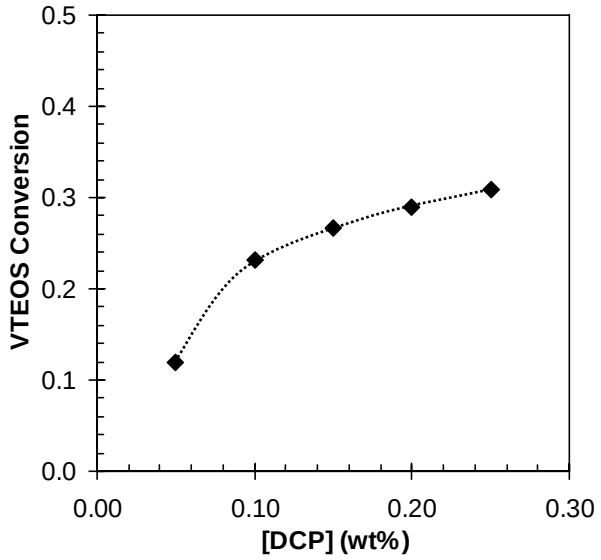

Figure 2.4: Ultimate VTEOS conversion to grafts as a function of peroxide loading (LLDPE, [VTEOS] = 5.0 wt%; T = 153°C)

The monomer conversions recorded in LLDPE modification experiments were sensitive to initiator loading, but they were relatively unaffected by the reaction

temperature (Figure 2.5). This is consistent with the model hydrocarbon results presented in Figures 2.2 and 2.3. Additional information regarding the outcome of LLDPE modifications is available in the form of complex viscosity (η^*) measurements. Figure 2.5 shows that η^* values recorded at a given peroxide loading were virtually constant, indicating that the crosslink density incurred as a result of graft-modification was also independent of the grafting temperature. Since, LLDPE crosslinking is derived from macroradical combination [14], the invariability of η^* suggests that temperature had little effect on alkyl macroradical yields, and by extension, on initiation efficiency.

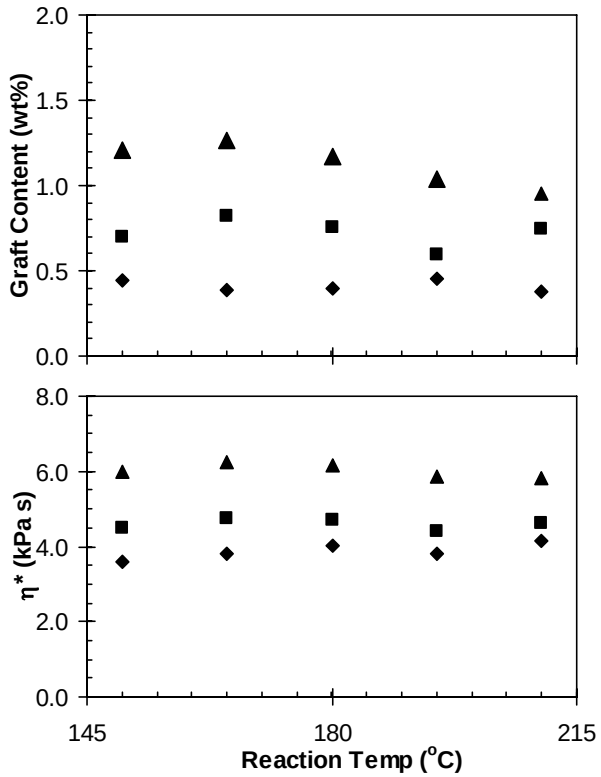

Figure 2.5: Silane graft content and complex viscosity of LLDPE-g-VTEOS ([VTEOS] = 5 wt%; ▲: [DCP] = 0.10 wt; ■: [DCP] = 0.05 wt%; ◆: [DCP] = 0.025 wt%)

A final series of LLDPE modification trials are summarized in Table 2.1. These experiments illustrate the generality of the observed temperature insensitivity in terms of peroxide type and, by extension, initiator decomposition rates. Further insight has been gained from moisture-cured gel content measurements for each sample, since the extent of a moisture-cure is dependent not only on the silane graft content of the material, but also on the distribution of these grafts within, and between, polymer chains.

Scheme 2.1 illustrates the main propagation reactions that govern the composition distribution of VTEOS-modified LLDPE. The balance of intramolecular and intermolecular abstraction rates by the VTEOS-derived adduct radical (V·) exerts the greatest influence on the placement of successive silane grafts [6]. If this balance were to shift with temperature, then the distribution of grafts amongst, and within, polymer chains would be altered. The gel content data presented in Table 2.1 show little variation for a given peroxide. We conclude that the composition distribution of LLDPE-g-VTEOS is not a strong function of temperature.

Table 2.1 Properties of LLDPE-g-VTEOS prepared using DCP, L-101 and L-130[a]

	0.05 wt% DCP			0.05 wt% L-101			0.05 wt% L-130		
Temp ^{o}C	η* kPa s[b]	Graft Content (wt %)	Cured Gel Content[c] (wt %)	η* kPa s[b]	Graft Content (wt %)	Cured Gel Content[c] (wt %)	η* kPa s[b]	Graft Content (wt %)	Cured Gel Content[c] (wt %)
150	4.50	0.7	90	5.89	1.1	90	----	----	----
165	4.77	0.8	80	5.75	1.1	90	5.89	0.8	90
180	4.71	0.8	80	5.54	1.0	90	5.29	0.9	90
195	4.41	0.8	75	5.44	1.2	95	5.49	0.8	90
210	4.64	0.7	80	5.33	1.0	90	5.53	1.0	90
225	----	----	----	----	----	----	5.30	0.9	95

a. 5 wt% VTEOS.

b. 180°C, 1 Hz, 3° arc.

c. Moisture-cured following graft modification.

L-101: 2,5-dimethyl-2,5-di(*tert*-butyl peroxy)-hexane.

L-130: 2,5-diethyl-2,5-bis(*tert*-butyldioxy)-3-hexyne.

2.4 Discussion.

Detailed kinetic schemes and their accompanying rate expressions have been generated for radical-mediated graft copolymerizations involving polymerizable monomers [15, 16]. While these models are concerned primarily with homopolymerization rates and molecular weight distributions, neither of these issues is particularly important to polyethylene functionalizations involving VTEOS. In the first place, the activation of vinyltrialkoxysilanes by radical initiators leads to extensive chain transfer to monomer in the case of bulk VTEOS polymerizations [5], and to chain transfer to a hydrocarbon in the case of polyolefin graft modifications [6,7]. Therefore, vinylsilane homopolymerization can be ignored without introducing significant error to the analysis. Molecular weight changes are restricted to those stemming from macroradical combination, and although this affects melt viscosity, crosslinking is easily represented by existing kinetic schemes [17], and we will not examine this process explicitly.

A wide array of reactions may generate alkyl macroradicals (P·, Scheme 2.1). Simplified treatments of the initiation process attribute macroradical formation to hydrogen atom abstraction by the oxygen-centred radicals derived from peroxide homolysis. These electrophilic species [18] prefer hydrogen atom abstraction to addition to electron deficient olefins, whereas the opposite tendencies are observed for the nucleophilic methyl radicals derived from cumyloxy radical fragmentation [19,

20]. It is known that higher temperatures accelerate alkoxy radical fragmentation in DCP-initiated processes [21], but a complete understanding of initiation requires more than knowledge of the fate of cumyloxy radicals, and must include information regarding the reactivity of methyl radical intermediates. This information does not exist at present, thereby rendering incomplete any attempt to analyze the initiation process in detail.

The simplest model of initiation uses an initiation efficiency, *f*, to quantify the proportion of DCP-derived radicals that succeed in producing a propagating macroradical.

$$R_i = 2 f k_d [ROOR]_o e^{-k_d t} \qquad (1)$$

Based on the initiation pathways illustrated in Scheme 2.1, one might expect *f* to vary widely with temperature and monomer concentration. However, the LLDPE graft contents and viscosities plotted in Figure 2.5 and listed in Table 2.1 suggest that macroradical yields and, hence, overall initiation efficiencies, may be insensitive to temperature despite the apparent complexity of the initiation mechanism.

The challenges encountered when describing radical termination are akin to those faced in monomer copolymerization, in that a variety of macroradical species can be present in concentrations that vary with the reaction extent. Because of the reasonably high kinetic chain length of VTEOS grafting, we can restrict our analysis to termination reactions of polymer and monomer derived macroradicals P· and V·,

respectively (Scheme 2.1). A standard means of handling the termination of two radical species is to define a cross termination parameter, $\phi = k_{t,2} / 2(k_{t,1}\, k_{t,3})^{1/2}$, from overall rate constants (that include combination and disproportionation) for use in a compolymerization rate expression [22]. We note that ϕ often approaches unity, thereby reducing the expression to one in which a single rate constant, k_t, can be used to account for the kinetics of radical termination. In the present case, this approximation leads to the following rate equation.

$$\begin{aligned} R_t &= 2k_{t,1}[P\cdot]^2 + 2k_{t,2}[P\cdot][V\cdot] + 2k_{t,3}[V\cdot]^2 \\ &\approx 2k_t[P\cdot]^2 + 2(2k_t)[P\cdot][V\cdot] + 2k_t[V\cdot]^2 \\ &= 2k_t([P\cdot]+[V\cdot])^2 \end{aligned} \qquad (2)$$

We have adopted the convention used by others, in which the cross-termination process (P· + V·) is assigned a rate constant $k_{t,2} = 2k_t$ to acknowledge the greater statistical probability of this event [12, 23].

In sharp contrast to modification processes that involve extensive homopolymerization, graft propagation in the present system involves not only macroradical addition (P·) to monomer, but also hydrogen atom transfer to the resulting silane-derived radical (V·). The overall dynamics of grafting are, therefore, dependent on which element of the propagation cycle is rate determining, which may shift with VTEOS conversion (Scheme 2.1). While others have assigned either monomer addition [24] or hydrogen transfer [11] as rate-limiting, we wish to maintain sufficient generality in our kinetic scheme such that either eventuality is adequately described.

Graft formation results from hydrogen atom donation to V· according to the following rate expression.

$$\frac{d[\text{Grafts}]}{dt} = k_{tr,\,inter}[V\cdot][P-H] + k_{tr,\,intra}[V\cdot] + k_{tr,deg}[V\cdot]$$
$$= (k_{tr,\,inter}[P-H] + k_{tr,\,intra} + k_{tr,deg})[V\cdot]$$
$$= k_{tr}[V\cdot] \qquad (3)$$

where k_{tr} is an overall rate constant that encompasses intermolecular hydrogen transfer (k_{tr}[P-H]) and [P-H] is the concentration of polymer units that are available for hydrogen abstraction, which can be treated as a constant, intramolecular abstraction ($k_{tr,intra}$) and degradative chain transfer to ethoxy groups ($k_{tr,deg}$). The composition distribution of VTEOS-modified resins is dictated largely by the balance established by these hydrogen atom transfer reactions. Model studies of VTEOS grafting [7], as well as fundamental studies of competitive inter- and intra-molecular hydrogen abstractions [25, 26], suggest that intramolecular processes can be dominant. Degradative chain transfer can be extensive in bulk homopolymerizations of VTEOS [4, 5], but its frequency is reported to be considerably reduced under hydrocarbon graft-modification conditions [6].

Whereas graft formation abides by equation 3, VTEOS is consumed through alkyl macroradical attack. Assuming that degradative chain transfer is a relatively minor pathway, monomer consumption can be described by considering only additions of P· according to equation 4.

$$-\frac{d[\text{VTEOS}]}{dt} = k_g[P\cdot][\text{VTEOS}] \qquad (4)$$

VTEOS consumption and graft formation is very likely to generate a pseudo-steady state condition, leading to a simple expression for overall grafting rate, R_g.

$$R_g = k_g[P\cdot][VTEOS] = k_{tr}[V\cdot] \quad (5)$$

In order to transform R_g into a function of measurable or estimable process variables, we require knowledge of the relationship between the concentrations of P· and V·. Rather than assuming that V· is produced in proportion to P· [27], we have chosen to evaluate a material balance on the overall macroradical population, which is governed by R_i and R_t. By applying a steady state assumption to equations 1 and 2, we generate

$$2fk_d[ROOR]_o e^{-k_d t} = 2k_t([P\cdot]+[V\cdot])^2$$

or

$$([P\cdot]+[V\cdot]) = \sqrt{\frac{fk_d[ROOR]_o}{k_t}} e^{-\frac{k_d}{2}t} \quad (6)$$

which, when applied to equation 5, gives the instantaneous rate of graft formation.

$$R_g = \frac{k_g[VTEOS]k_{tr}}{k_g[VTEOS]+k_{tr}} \sqrt{\frac{fk_d[ROOR]_o}{k_t}} e^{-\frac{k_d}{2}t} \quad (7)$$

Since this expression does not assign a rate determining step to the propagation sequence, it represents VTEOS grafting dynamics over the whole range of monomer conversion. The reaction order with respect to VTEOS concentration may range from 0 to 1 depending upon the relative magnitudes of k_{tr} and k_g, as well as the concentration of VTEOS in the system.

The predicted evolution of R_g with time is also interesting, as it is dictated by a time

constant of $k_d/2$. Non-chain processes such as polyolefin crosslinking follow first-order kinetics with a time constant of k_d, and can therefore be considered complete after six initiator half-lives. In contrast, graft addition is dictated by a time constant one-half of k_d, and significant amounts of grafting can occur beyond this threshold. The kinetic chain length for grafting, defined as R_g/R_t, illustrates this argument more concisely.

$$KCL = R_g/R_t = \frac{k_g[VTEOS]k_{tr}}{k_g[VTEOS] + k_{tr}} \frac{1}{2\sqrt{fk_d[ROOR]_o}} e^{\frac{k_d}{2}t} \qquad (8)$$

The exponential rise of KCL with time reflects the first-order dependence of R_g on macroradical concentration, versus the second-order dependence of R_t on this variable. Consequently, a drop in radical concentration creates a corresponding increase in radical lifetime, and enhances the number of grafts that follow from each successful initiation event.

The instantaneous rate expression is easily integrated from t=0, $[VTEOS]=[VTEOS]_o$ to any time, t, to yield equation 9.

$$\frac{1}{k_{tr}}([VTEOS]_o - [VTEOS]) + \frac{1}{k_g}\ln\frac{[VTEOS]_o}{[VTEOS]} = 2\sqrt{\frac{f[ROOR]_o}{k_d k_t}}(1 - e^{-\frac{k_d}{2}t}) \qquad (9)$$

In terms of VTEOS conversion, $X = ([VTEOS]_o-[VTEOS])/[VTEOS]_o$, the dynamics of graft evolution follow equation 10.

$$\frac{[VTEOS]_o X}{k_{tr}} - \frac{1}{k_g}\ln(1 - X) = 2\sqrt{\frac{f[ROOR]_o}{k_d k_t}}(1 - e^{-\frac{k_d}{2}t}) \qquad (10)$$

Since the rate constant for DCP homolysis is known, the application of this expression to VTEOS conversion profiles requires estimates of three parameters (k_{tr}, k_g, and f /

k_t). While no experimental values are available, Russell has examined similar parameters for hydrocarbon maleation, and has judged $k_g = 5.0 \times 10^5$ $M^{-1}s^{-1}$, and $f / k_t = 0.5/3.0 \times 10^8$ $M^{-1}s^{-1} = 1.67 \times 10^{-9}$ M s as reasonable, order-of-magnitude estimates [12]. Starting with these values, a least-squares regression of equation 10 to the kinetic and yield data presented in Figures 1 and 2 produced a parameter estimate of $k_{tr} = 3.2 \times 10^3$ s^{-1}. Note that the objective of this fitting exercise was not to generate precise values for the model parameters, but to illustrate the capability of the derived rate expression to capture the dynamics and yields of VTEOS grafting processes. The solid lines drawn in Figures 1 and 2 are calculated using equation 10 with the regressed constants, and they show good agreement with experiment. It is clear, however, that these parameter estimates relate only to the model system, and the application of equation 10 to polyolefin modifications requires independent parameter evaluations.

We conclude our discussion with an examination of the temperature dependence of silane graft yields. Taking the limit of equation 10 to infinite time, the final VTEOS conversion (X_∞) can be expressed as follows.

$$\frac{\sqrt{k_d}}{k_{tr}}[\text{VTEOS}]_o X_\infty - \frac{\sqrt{k_d}}{k_g}\ln(1 - X_\infty) = 2\sqrt{\frac{f[\text{ROOR}]_o}{k_t}} \qquad (11)$$

The right hand side of equation 11 may be invariant with temperature, since recorded η^* values were relatively constant, and radical termination processes demonstrate very low activation energies [28]. If the rate constants for peroxide homolysis (k_d), radical addition to VTEOS (k_g) and overall hydrogen atom transfer events (k_{tr}) are rewritten according to an Arrhenius expression, $k_i = A_i \exp(-E_{a,i}/RT)$, we arrive at

equation 12.

$$\frac{\sqrt{A_d}}{A_{tr}} \exp\frac{(E_{A,tr} - E_{A,d}/2)}{RT}[VTEOS]_o X_\infty - \frac{\sqrt{A_d}}{A_g} \exp\frac{(E_{A,g} - E_{A,d}/2)}{RT} \ln(1 - X_\infty) = 2\sqrt{\frac{f[ROOR]_o}{k_t}} \qquad (12)$$

The activation energy for the rate determining step of propagation ($E_{A,tr}$ or $E_{A,g}$) need only equal half the value for peroxide homolysis ($E_{A,d}$) for graft yields to be independent of temperature. The activation energy for dicumyl peroxide homolysis ($E_{A,d}$) is approximately 159 kJ/mole, but there is no similar information available for the addition and hydrogen transfer reactions that support high-temperature VTEOS grafting processes. We note, however, that alkyl radical additions to olefins generally exhibit activation energies below 20 kJ/mole, with the addition of *tert*-butyl radicals to VTEOS having a reported activation energy of just 16.0 kJ/mole [22]. Hydrogen atom transfers can present more substantial activation energy barriers, reaching 42.4 kJ/mole for the gas-phase reaction of methyl radicals with propane [29]. Based on these approximate values, one would expect VTEOS graft yields to decline with temperature, which is not consistent with our experimental findings. Fundamental research on addition and hydrogen transfer reactions at graft-modification conditions would be of considerable value to this analysis, as would information on peroxide initiation efficiency and its variation with reaction temperature.

2.5 References and notes.

1. This chapter constitutes part of the published work: Parent, J.S.; Parodi, R and Wu, W.; *Polym. Eng. Sci.*, **2006**, *46*, 1754-1761.
2. Moad, G., *Prog. Polym. Sci.*, **1999**, *24*, 81-142.
3. Ganzeveld, K.J. and Janssen, L.P.B.M., *Polym. Eng. Sci.*, **1992**, *32*, 467-474.
4. Isac, S. and George, K.E., *Plast. Rubber Compos.*, **2001**, *30*, 34-38.
5. Mixer, R.Y. and Bailey, D.L., *J. Polym. Sci.*, **1955**, *18*, 573-582.
6. Seyferth, D.; Son, D.Y. and M. Tasi, *Organometallics*, **1995**, *14*, 2225-2231.
7. Spencer, M.; Parent, J.S. and Whitney, R.A., *Polymer*, **2003**, *44*, 2015-2023.
8. Forsyth, J.C.; Baker, W.E.; Russell, K.E. and Whitney, R.A., *J. Polym. Sci. Part A: Polym. Chem.*, **1997**, *35*, 3517-3525.
9. Parent, J.S.; Tripp, M. and Dupont, J., *Polym. Eng. Sci.*, **2003**, *43*, 234-242.
10. Heinen, W.; Rosenmoller, C.H.; Wenzel, C.B.; de Groot, H.J.M.; Lugtenburg, J. and van Duin, M. *Macromolecules*, **1996**, 29, 1151-1157.
11. Russell, K.E. *J. Polym. Sci. Part A: Polym. Chem.*, **1988**, *26*, 2273-2280.
12. Sipos, A.; McCarthy, J. and Russell, K.E., *J. Polym. Sci. Part A: Polym. Chem.*, **1989**, *27*, 3353-3362.
13. Russell, K.E., *Prog. Polym. Sci.*, **2002**, *27*, 1007-1038.
14. Van Drumpt, J.D. and Oosterwijk, H.H.J., *J. Polym. Sci. Part A: Polym. Chem.*, **1976**, *14*, 1495-1511.
15. Huang, N.J. and Sundberg, D.C., *J. Polym. Sci.: Part A: Polym. Chem.*, **1995**, *33*, 2533-2549.

16. Manaresi, P.; Passalacqua,V. and Pilati, F., *Polymer*, **1975**, *16*, 520-526.

17. Lazar, M., *Adv. Polym. Sci.*, **1989**, *5*, 149-223, and references therein.

18. Minisci, F. and Galli, R., *Tetrahedron Letters*, **1962**, *12*, 533-538.

19. Ingold, K.U., *Free Radicals. Vol. 1*, Kochi, J.K. ed., Wiley, **1973**, pg 92.

20. Zytowski, T. and Fischer, H., *J. Amer. Chem. Soc.* **1997**, *119*, 12869-12878.

21. Chodak, I. and Bakos, D., *Coll. Czech. Chem. Commun*, **1976**, *43*, 2574-2577.

22. Rudin, A., *Elements of Polymer Science and Engineering*, Academic Press, San Diego, **1982**, pg. 295.

23. Munger, K. and Fischer, H., *Int. J. Chem. Kinetics*, **1985**, *17*, 809-829.

24. Sen, A. K.; Mukherjee, B.; Bhattacharyy, A.S.; De, P.P. and Bhowmick, A.K., *J. Appl. Polym. Sci.*, **1992**, *44*, 1153-1164.

25. Wilt, J.W., In: *Free Radicals, Vol.1*, Kochi J.K., editor. J. Wiley & Sons: New York, **1973**, 333-502.

26. Rust, F.F., *J. Am. Chem. Soc.*, **1957**, *79*, 4000-4003.

27. Cha, J. and White, J.L., *Polym. Eng. Sci.*, **2001**, *41*, 1227-1237.

28. Gibian, M.J. and Corely, R.C., *Chem. Rev.*, **1973**, *73*, 441-464.

29. Tedder, J.M., *Tetrahedron*, **1982**, *38*, 313-329.

Chapter 3: Bicumene Initiated Graft Modification of Hydrocarbons[1]

3.1 Introduction

The radical-mediated addition of vinyltriethoxysilane (VTEOS) to polyolefins is typically initiated using alkyl peroxides, whose oxygen-centred radical products provide a favourable balance between hydrogen atom abstraction and monomer addition [2]. Single-screw extrusion experiments have recently been described wherein 2,3-dimethyl-2,3-diphenyl butane, or bicumene, was used as a radical initiator at temperatures ranging from 220°C to 290°C [3]. Since this range cannot be accessed using commercially available peroxides, bicumene provides an entry into a temperature domain where the rates of monomer addition, hydrogen atom abstraction and macroradical fragmentation may be quite different than those provided by conventional grafting operations.

Two important advantages may follow from these differences. In the first place, the kinetic chain length for VTEOS addition, which is defined as the number of grafts produced by each macroradical initiated, may be enhanced by operating at higher temperature. This measure of grafting performance is dictated by the relative rates of graft propagation and radical termination [4]. Given the relatively high activation energy of the radical addition and hydrogen transfer reactions that constitute a graft propagation sequence, a high operating temperature may disproportionately accelerate graft formation over radical termination. A second potential advantage relates to

reaction selectivity. Whereas conventional vinylsilane additions to ethylene-rich polyolefins produce significant levels of crosslinking, a bicumene-based process may provide a means of inducing macroradical fragmentation such that the influence of radical combination on molecular weight is offset, thereby decoupling graft contents from molecular weight effects.

That bicumene can support a reactive extrusion process is somewhat surprising, given the exceptionally long half-life of this initiator [5], and the reportedly poor hydrogen-atom abstraction capacity of the resonance-stabilized, cumyl radicals derived from bicumene homolysis [6]. Based on extrusion experiments and limited analyses of bicumene-derived products, it has been suggested that initiation could involve an air-oxidation mechanism, wherein cumyl radical intermediates lead to oxygen-centred species whose hydrogen abstraction efficiency is adequate for the purposes of graft initiation [2]. Due to difficulties in controlling the environment of polymer grafting experiments, the intrinsic initiation activity of bicumene in the absence of oxygen has not been established, nor has the importance of an oxidative initiation pathway.

The objective of this work was to characterize the dynamics of bicumene initiation under controlled conditions, and to generate unambiguous information regarding the initiation mechanism. To this end, isothermal batch experiments that define the effect of temperature and bicumene concentration on hydrocarbon graft modification

are described and interpreted to develop and validate a plausible initiation mechanism.

3.2 Experimental

Materials. 2,3-Dimethyl-2,3-diphenylbutane (bicumene, Perkadox-30, 95%, Akzo Nobel) and vinyltriethoxysilane (97%, VTEOS, Sigma Aldrich) were used as received.

Analysis. ^{1}H-NMR spectra were recorded in $CDCl_3$ using a Bruker AC-400 spectrometer, with chemical shifts reported in ppm relative to chloroform (δ 7.24).

VTEOS Grafting to Cyclooctane. Stock solutions (5 ml) of cyclooctane, VTEOS (5 wt%) and the required amount of bicumene were charged to a series of 10 ml stainless steel bombs and deoxygenated to differing degrees by pressurizing with high-purity nitrogen to 1.5 MPa, mixing, and releasing for a total of 0, 1, 2, 4 and 8 cycles, depending on the desired oxygen partial pressure. After deoxygenation, each bomb was sealed under 1.5 MPa of N_2 and immersed in an oil bath at the desired temperature under constant magnetic stirring. Crude reaction products were analyzed by ^{1}H-NMR to determine the conversion of VTEOS to grafts by comparison of residual olefin resonances to the methylene groups of the alkoxysilane functionality and the aliphatic resonances derived from cyclooctane. Reported partial pressures (P_{O2}) represent the pressure of oxygen within the sample bomb at room temperature.

Bicumene Decomposition. Solutions of 5 wt% bicumene in the desired hydrocarbon were charged to stainless steel bombs and deoxygenated before pressurizing to 1.5 MPa with N_2 and heating to 240°C for 2 hours. ^{1}H-NMR and gas chromatography (GC) were used to determine product concentrations. GC analysis employed a Supelco SPB-1 microbore column, with injector and detector temperatures of 225 and 300 °C, respectively. The oven temperature profile involved 40 °C for 6 min, ramping to 150 °C at 10 °C/min, ramping to 280 °C at 12 °C/min, and holding for 15 min. Helium carrier gas was used at 2 ml/min. Calibrations of retention time and flame ionization detector response were developed for α-methylstyrene, acetophenone, cumyl alcohol, cyclooctanone, cyclooctanol, and bicumene using authentic samples. The ratio of cumene to α-methylstyrene was determined by ^{1}H-NMR spectrum integration using resonances at δ 2.90 ppm (m, 1H, CH) for cumene and δ 5.06 ppm (s, 1H, =CH) for α-methylstyrene.

3.3. Results

3.3.1 Fundamentals of Bicumene Initiation

It is exceedingly difficult to control the concentration of O_2 in polymer modification processes, but it is a simple matter to manipulate the environment of small-molecule reactions. Insight into the nature of bicumene initiation has been gained by examining the addition of VTEOS to cyclooctane. The use of a cyclic hydrocarbon facilitates detailed structural characterizations, but it is known that cyclooctane

engages more readily in hydrogen atom donation than acyclic hydrocarbons [7]. Given the focus on determining the primary mode of bicumene activation, this difference was not critical, but where issues relating to substrate reactivity were concerned, the behaviour of acyclic model hydrocarbons has been examined.

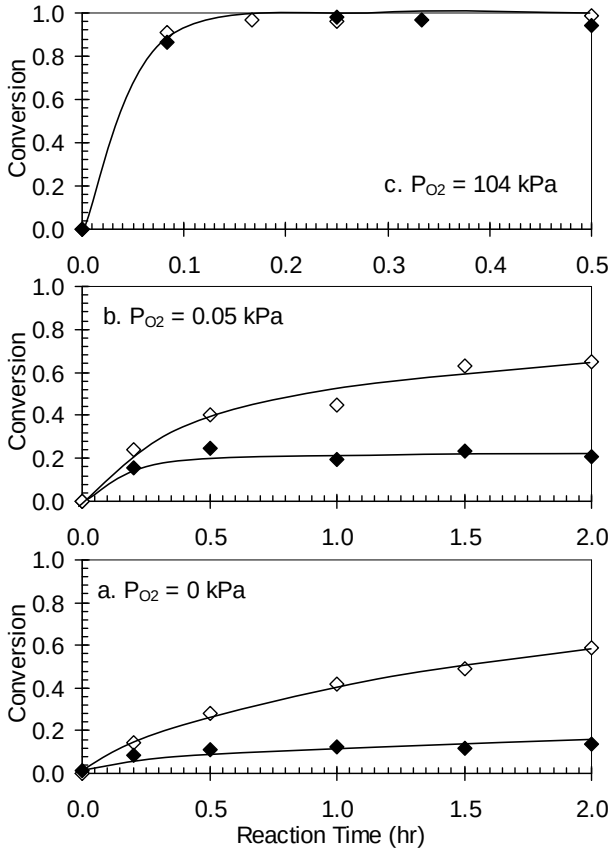

Figure 3.1 Dynamics of VTEOS grafting to cyclooctane as a function of P_{O2} (T=240°C; 5 wt% VTEOS; P_{total} = 1500 kPa; ◆: no bicumene; ◇: 0.10 wt% bicumene).

The dynamics of a series of cyclooctane modifications, each conducted under a different partial pressure of oxygen (P_{O2}) or bicumene concentration, are illustrated in Figure 3.1. The data confirm that bicumene can initiate VTEOS grafting to hydrocarbons under oxygen-free conditions (Figure 3.1a). After 2 hours at 240°C, a

reaction mixture containing 0.10 wt% bicumene yielded a VTEOS conversion of 59%. This performance is comparable to that observed graft modifications of tetradecane and cyclohexane under deoxygenated conditions. Therefore, the intrinsic (oxygen-free) ability of bicumene to initiate grafting is not substrate specific, and a complete initiation mechanism must provide direct pathways for the activation of the hydrocarbon by cumyl radicals.

Further insight into the initiation mechanism has been gained by examining bicumene decomposition rates and byproducts in the absence of VTEOS. When heated to 240°C in trichlorobenzene and deuterated octane, bicumene yielded α-methyl styrene (α-MeSty) and cumene in a 1:1 ratio. Neither solvent is appreciably reactive with respect to radical attack due to the high bond dissociation energies encountered in aromatic compounds, and to the large kinetic isotope effects associated with deuterium abstraction [8]. With no effective donors present, and no fragmentation pathways available, cumyl radical disproportionation to the observed products is the only discernible reaction outcome (Scheme 3.1). An alternate fate is combination to regenerate bicumene, and since this termination reaction is more than an order of magnitude faster than cumyl radical disproportionation [9], the reversibility of bicumene homolysis cannot be ignored, as is common practice for peroxide initiators. Previous studies of bicumene decomposition rates confirmed the 8.2 hour half-life of bicumene in trichlorobenzene at 240°C, but also revealed a 2.3 hour half-life when benzenethiol is charged to the system [2]. This dramatic acceleration of bicumene

decomposition stems from the provision of a competitive hydrogen atom transfer pathway that is capable of quenching cumyl radicals irreversibly.

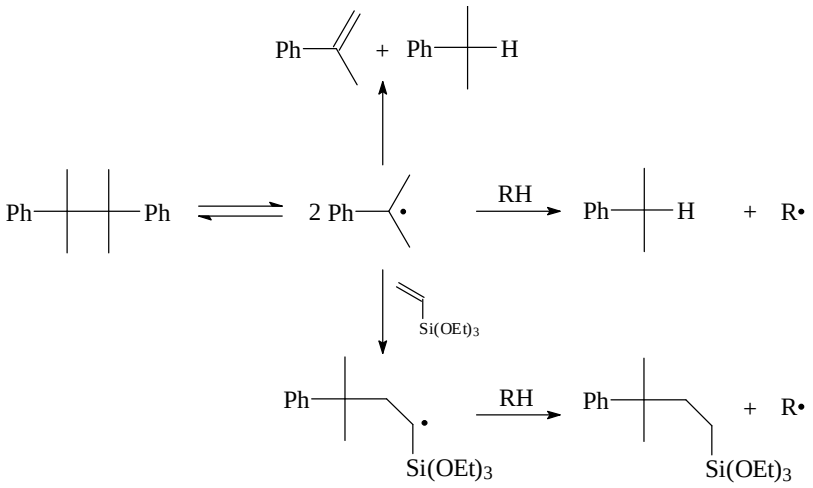

Scheme 3.1 Potential oxygen-free initiation pathways of bicumene.

Table 3.1 provides new information regarding bicumene decomposition in cylcooctane. The data show that 2 hours at 240°C was sufficient to consume approximately 50% of bicumene. This single-point estimate of bicumene half-life is comparable with that recorded in trichlorobenzene solutions containing benzenethiol, and it suggests that cyclooctane can serve as a hydrogen atom donor when present in high concentration. Evidence to support this claim is provided by the composition of bicumene decomposition products. The α-MeSty:cumene ratio was not 1:1 as observed for aromatic and deuterated solvents. Rather, the average ratio in cyclooctane was 1:4.3, and the values recorded for bicumene decompositions in n-octane and cyclohexane were both 1:1.7. The higher value recorded for cyclooctane is a direct result of the unique reactivity of this cyclic hydrocarbon to hydrogen atom donation, as noted above [6]. The reported C-H bond dissociation

energy of cyclooctane is 10.6 kJ/mole less than that of cyclohexane [10], resulting in much higher rates of hydrogen transfer to $Cl_3C\cdot$ radicals in gas [11] and liquid [6] phase reactions, and to elevated reactivity in hydrocarbon oxidations [12]. We note that, irrespective of the substrate, an abundance of cumene relative to α-methyl styrene is consistent with an initiation mechanism involving hydrogen atom abstraction by cumyl radicals.

Table 3.1: Bicumene and cyclooctane decomposition and/or oxidation byproducts (ppm)

P_{O2}	0 kPa	1.4 kPa	82 kPa
Bicumene Conversion	49%	54%	47%
Cumene	2190	2420	2020
α-MeStyrene	470	460	430
Cumyl Alcohol	0	50	180
Acetophenone	0	0	0
Cyclooctanol	0	230	4480
Cyclooctanone	0	150	2570
Octanal	0	0	0
Octanoic Acid	0	0	0

T=240°C; P_{total}=1500 kPa; 5 wt% bicumene in cyclooctane; 120 min.

While it is clear that oxygen is not required to activate bicumene for grafting purposes, its presence can have a remarkable effect on initiation activity. A small increase in the initial rate of VTEOS grafting to cyclooctane was observed under an O_2 partial

pressure of 0.05 kPa (Figure 3.1b), and a dramatic improvement was realized by operating with P_{O2} = 104 kPa (Figure 3.1c). In the latter case, 97% of VTEOS was converted within 17 min. Furthermore, no bicumene was required under these more forcing conditions, presumably due to the emergence of an auto-oxidation chain process, whose strength was such that additional radical sources were not required to sustain VTEOS addition.

The sensitivity of high-temperature grafting to the presence of oxygen is further demonstrated by Figure 3.2, in which the VTEOS conversion recorded after 10 min of reaction time is plotted as a function of P_{O2}. Deoxygenated reaction conditions (P_{O2} 〈 0.1 Pa) converted 20% of VTEOS to grafts, and a higher oxygen partial pressure of 0.05 kPa had little effect. However, beyond this threshold partial pressure, grafting activity increased sharply, and the necessity of bicumene declined in equal measure.

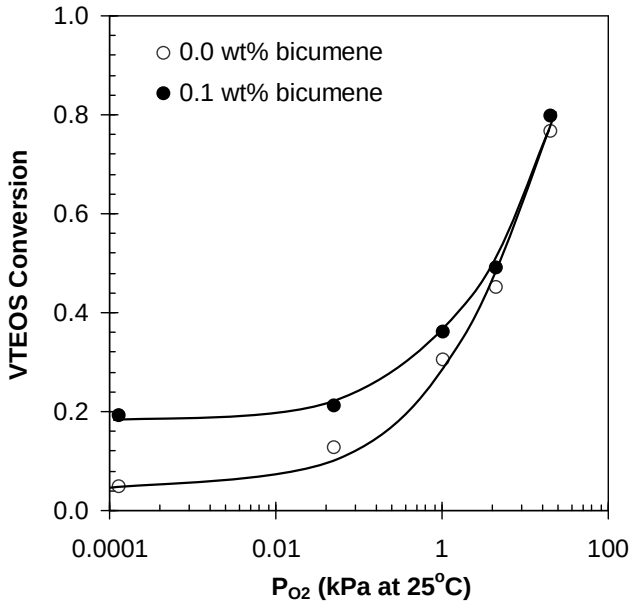

Figure 3. 2: VTEOS conversion to cyclooctane grafts as a function of O_2 partial pressure (240°C; 10 min; P_{total} = 1500 kPa).

3.4. Discussion

3.4.1 Grafting Under Oxygen-free Conditions

It is clear that the slow decomposition of bicumene to yield cumyl radicals of relatively low hydrogen atom abstraction potential can contribute only a small population of polymer macroradicals to a grafting process that operates at 240°C. Nevertheless, a substantial amount of VTEOS grafting has been achieved at this temperature using bicumene at levels as low as 0.05 wt%. If a small radical population is to generate a significant amount of monomer addition, the graft propagation sequence must operate with a kinetic chain length that is substantially greater than that observed in conventional peroxide-initiated reactions that function at comparatively low temperature.

Consider the simplified grafting mechanism illustrated in Scheme 3.2. Graft modification involves both VTEOS addition to polymer macroradicals and hydrogen atom abstraction (either intra- or inter-molecular) to generate a silane graft. Since there is no information regarding the relative rates of these components of the propagation sequence, it is not known whether the polymer macroradical (P·) or the vinylsilane adduct (A·) is the dominant chain-carrying species. Nevertheless, whichever intermediate predominates, radical combination and disproportionation will terminate the propagation sequence. Therefore, a kinetic chain length derived from the rate of graft propagation divided by the rate of radical termination will be

proportional to $k_{prop}/(k_{term}[R\cdot])$, where k_{prop} is the constant for the rate limiting step of the propagation sequence, k_{term} is the overall radical termination constant, and $[R\cdot]$ is the instantaneous radical concentration.

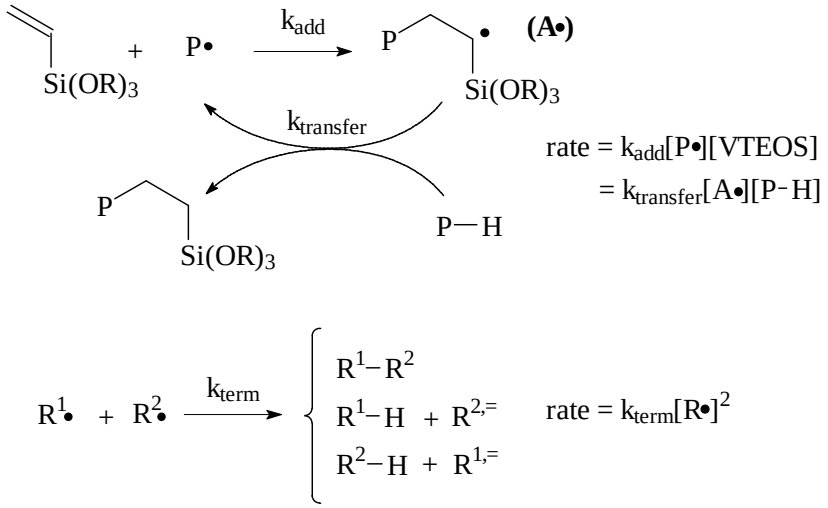

Scheme 3.2: Simplified graft propagation and termination pathways for VTEOS grafting

It is plausible that the extraordinary kinetic chain length provided by a bicumene-based process may be the product of a high propagation rate constant, and a low steady-state radical population. The first assumption stems from the relatively high activation energy for graft propagation compared to that of radical termination. Radical termination proceeds at rates that approach their collision frequency and, as a result, the process presents a minimal activation energy barrier irrespective of the mode of termination [13]. In contrast, the addition of a *tert*-butyl radical to VTEOS requires that an activation energy of 16 kJ/mole be overcome [14], while hydrogen atom transfer between alkyl radicals can present energy barriers of this order of

magnitude [15]. Therefore, as temperatures are raised from conventional values such as 190°C to the levels employed in this work, an increase in the kprop/kterm ratio will have a positive effect on kinetic chain length.

The radical concentration established by a given initiator is equally important. Rapid initiator decomposition leads to high instantaneous radical concentrations, thereby increasing the frequency of radical termination events, reducing radical lifetimes, and decreasing kinetic chain lengths. At temperatures above 240°C, the homolysis of standard peroxides is so rapid that benefits gained from heightened propagation rates may be offset by a corresponding increase in [R·], and by extension, in the radical termination rate. By delivering a small, but steady, radical population, bicumene may exploit the benefits of high temperature grafting without incurring difficulties associated with rapid initiator decomposition.

3.4.2 Oxidation-enhanced initiation

The accelerated grafting rates observed when bicumene is activated by oxygen are explained by well-established principles of hydrocarbon oxidation [16, 17]. The trapping of carbon-centred radicals by O_2, which may be reversible in the case of cumyl radicals, [18] can support an auto-accelerating reaction sequence that generates several oxygen-centred radicals from a single alkyl radical. The hydroperoxide intermediates that are isolable in low-temperature oxidations [19] were not found

within reaction products, presumably due to their sensitivity to the temperatures used in this work and to trace metal impurities within our system [20].

Oxygen trapping is not restricted to cumyl radicals, and hydrocarbon oxidation products were found in model compound experiments that employed modest O_2 pressures (Table 3.1). Cyclooctanol was the dominant byproduct, whose formation is rationalized by the same oxidation mechanisms cited above. The most direct route to a ketone byproduct involves disproportionation of secondary alkylperoxyl and/or alkoxyl radicals (Scheme 3.3) [21] but hydrogen abstraction from cyclooctanol may lead to the corresponding hydroperoxide, that would in turn establish an equilibrium with the observed ketone and H_2O_2 [22].

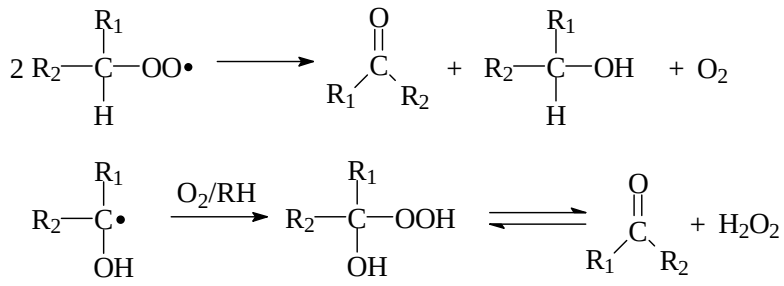

Scheme 3. 3: Pathways for the production of cyclooctanone.

Although oxygen is not strictly required for bicumene to initiate VTEOS additions, the extent to which oxidation might contribute to bicumene-initiated HDPE modification is difficult to assess. The solubility of oxygen in PE at the temperatures of interest is unknown. But, if it is assumed that all of the oxygen available to a PE grafting process is contained in the semi-crystalline polymer at 25°C,

this would amount to an upper limit of 30μM of O_2 to be contained in the polymer melt [23]. To produce this oxygen concentration in cyclooctane at 25°C requires an oxygen partial pressure of about 0.4 kPa [24]. The data presented in Figure 3.2 show that this level of oxygen has a marginal effect on VTEOS graft yields, and this suggests that oxidative mechanisms contribute only to a small degree.

3.5. Conclusions

Bicumene homolysis generates a macroradical population that is effective for the graft modification of hydrocarbons. The high-temperatures supported by this process accelerate the graft propagation sequence, thereby improving the kinetic chain length of VTEOS additions.

3.6 References and notes.

1. This chapter consititutes part of the published manuscript: Parent, J.S.; Wu, W.; Sengupta, S.S.; Jackson, P., *Eur. Polym. J.*, **2006**, *42*, 971-980.
2. Moad, G. *Prog Polym Sci.*, **1999**, *24*, 81-142.
3. Parent, J.S.; Cirtwill, S.; Penciu, A.; Whitney, R, A.; and Jackson, P., *Polymer*, **2003**, *44*, 953-961.
4. Russell, K.E.; *Prog. Polym. Sci.*, **2002**, *27*, 1007-1038.
5. In: Brandrup, J.; Immergut, E.H. and Grulke, E.A., editors. *Polymer Handbook*, 4th edition, New York: Wiley, **1999**, pg. II-68.

6. The C-H bond dissociation energy of cumene is 353.1 kJ/mole, compared to 399.6 kJ/mole for cyclohexane.
7. Alfassi, Z.B. and Feldman, L., *Int. J. Chem. Kinet.* **1981**, *13*, 517-526.
8. Fujisaki, N.; Ruf, A. and Gaumann, T., *J. Chem. Phys.*, **1984**, *80*, 2570-2577.
9. Nelsen, S.F. and Bartlett, P.D., *J. Amer. Chem. Soc.*, **1966**, *88*, 137-143.
10. Fujisaki, N.; Ruf, A. and Gaumann, T., *J. Amer. Chem. Soc.*, **1985**, *107*, 1605-1610.
11. Wampler, F.B. and Kuntz, R.R., *Int. J. Chem. Kinet.*, **1971**, *3*, 283-289.
12. Cook, G.K. and Mayer, J.M., *J. Amer. Chem. Soc.*, **1995**, *117*, 7139-7156.
13. Gibian, M.J. and Corely, R.C., *Chem. Rev.*, **1973**, *73*, 441-464.
14. Muenger, K. and Fisher, H., *Int. J. Chem. Kinet.*, **1985**, *17*, 809-829.
15. Ingold, K.U., In: J. K. Kochi, editor. *Free Radicals*, Volume I, New York: J Wiley & Sons, **1973**, pp. 37-112.
16. Howard, J.A.; Bennett, J.E. and Brunton, G., *Can. J. Chem.*, **1981**, *59*, 2253-2260.
17. Bell, E.R.; Raley, J.H.; Rust, F.F.; Seubold, F.H. and Vaughan, W.E., *Discussions Faraday Soc.*, **1951**, *10*, 242-249.
18. Benson, S.W., *J. Amer. Chem. Soc.*, **1965**, *87*, 972-979.
19. Walling, C., *J. Amer. Chem. Soc.*, **1969**, *91*, 7590-7594.
20. Kharasch, M.S.; Fono, A. and Nudenberg, W., *J. Org. Chem.*, **1951**, *16*, 113-127.
21. Tolman, C.A.; Druliner, J.D.; Nappa, M.J. and Herron, N., *Activation and Functionalization of Alkanes*, 303-360, edited by Hill, C.L., **1989**; John Wiley & Sons.

22. Brown, N.; Hartig, M. J.; Roedel, M. J.; Anderson, A.W. and Schweitzer, C.E., *J. Amer. Chem. Soc.*, **1955**, *77*, 1756-1759.

23. Michaels, A. and Bixler, H.J., *J. Polym. Sci.*, **1961**, *50*, 393-412.

24. Wilcock, R.J.; Battino, R. and Wilhelm, E.J., *Chem. Thermodynamics*, **1977**, *9*, 111-115.

Chapter 4: Polymer Functionalization by Free Radical Addition to Alkynes[1]

4.1 Introduction.

As noted in previous chapters, the free radical addition of saturated polymers to monomers such as maleic anhydride and vinyltrialkoxysilanes yields functional derivatives that are valued for blend compatibilization and filler reinforcement applications.[2, 3] These solvent-free, peroxide-initiated processes exploit a closed sequence of macro-radical addition to C=C unsaturation, and hydrogen atom abstraction from the polymer by the resulting alkyl radical adduct. An efficient propagation sequence produces single grafts with high kinetic chain lengths, such that initiator loadings - and the yield of crosslinking and/or fragmentation byproducts that are tied to initiator concentrations – can be closely regulated. [4, 5]

The advent of “click chemistry” has increased the availability of functional alkynes, leading us to examine them in the context of polymer graft modification. This subject has received no attention other than a report of acetylene’s ability to promote polyethylene cross-linking.[6] There is, however, is a substantial body of organic synthesis literature devoted to small molecule systems.[7, 8] Most examples are intra-molecular, stereo-selective cyclizations, [9, 10] but inter-molecular additions to acetylene have been demonstrated, leading to allylic alcohols, amines, esters and ketones. [11] Reaction yields reported for substituted alkynes are quite variable, with high temperature additions of cyclohexane being much less efficient [12] than

corresponding additions of $(Me_3Si)_3SiH$. [13]

The kinetic chain length of a polymer-alkyne reaction will be dictated by the rate of alkyl macro-radical addition to the carbon-carbon triple bond (k_{add}; Scheme 4.1), and/or the rate of hydrogen atom abstraction by the resulting vinyl radical (k_{tr}; Scheme 4.1). The rate constants reported for alkyl radical additions to mono-substituted alkynes are less than those observed for olefinic analogues.[14] For example, the attack of tert-butyl radicals on methyl acrylate occurs 6.2 times faster than on methyl propiolate at 27°C.[15] However, activation energies are significantly higher for alkyne additions, [16] suggesting that rates may be more attractive at the higher temperatures that are needed to modify semi-crystalline polymers. With respect to the hydrogen transfer component of graft propagation, abstraction by vinyl radicals from secondary alkyl groups is exothermic, and although thermodynamics alone do not dictate hydrogen transfer rates, the energetics of vinyl radical quenching by R-H donors are potentially more favourable than those encountered in the aforementioned maleation and vinylsilane processes.

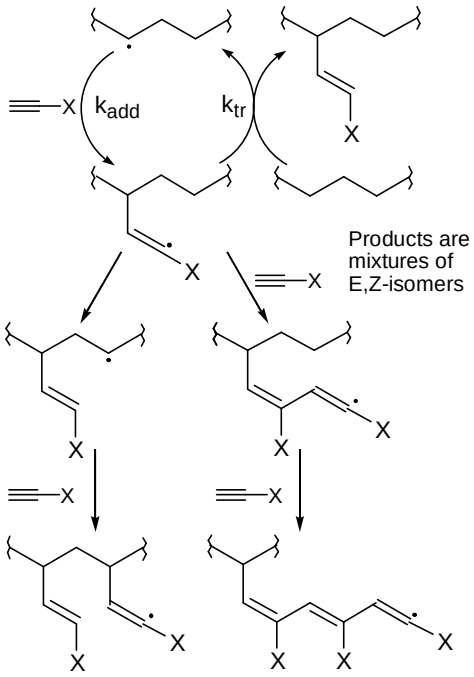

Scheme 4. 1 Expected reactions in radical initiatiated alkyne grafting.

The introduction of single, uniformly distributed grafts is desirable, but other propagation sequences may contribute to product distributions (Scheme 4.1). For example, intra-molecular 1,5-hydrogen atom transfer by intermediate vinyl radicals (radical translocation),[17] can lead to repeated functionalization of a given polymer chain, as will oligomerization of the modifier to produce polyene grafts.[18] Given that the initial products of alkyne addition are olefinic, alkynes may also serve as di-functional, cross-linking modifiers. The extent to which grafted moieties undergo radical attack will depend on the relative reactivity of mono-substituted alkynes versus di-substituted olefins and conjugated polyenes. That others have isolated mono-addition products in good yield suggests that these secondary reactions are not dominant. [6] Nevertheless, small amounts of modifier-induced cross-linking can exert great influence on the physical properties of a polymer system.

This report describes peroxide-initiated C-H bond addition to ethyl propiolate and phenyl acetylene at the reagent concentrations and reaction temperatures required for semi-crystalline polymer modifications. Insight gained from studies of the structure and yields of model hydrocarbon reactions is used to characterize polymer reaction products and to identify variables that affect alkyne conversions. The impact of alkyne addition on polymer molecular weight is also assessed.

4.2 Experimental

Materials. Dicumyl peroxide (99%, DCP), ethylpropiolate (99%, EP), phenylacetylene (98%, PhCCH) and cyclooctane (99%) were used as received from Sigma Aldrich. Poly(ethylene oxide) (PEO, Mv = 132 kg/mol) and polyethylene (PE, Mn=1.4 kg/mol) were used as received from Scientific Polymer Products.

Analysis. 1H-NMR spectra were recorded with a Bruker AC-400 spectrometer using $CDCl_3$ for model compounds and PEO derivatives, and toluene-d8 for PE derivatives. The solution viscosity of PEO-based materials was measured in chloroform at 25°C within a thermostated bath using an Ubbelhode viscometer that yielded elution times greater than 150 seconds, thereby eliminating the need for kinetic energy corrections. Data were acquired in the dilute solution region, and fit to the Huggins' equation $\eta_{red} = [\eta] + k_H [\eta]^2 c$, where $[\eta]$ is the intrinsic viscosity in ml/g, c is the polymer concentration in g/ml, and k_H is the empirical Huggins' parameter.[19]

Mono-disperse PEO standards with number average molecular weights of 33,600, 101,200, 246,600 and 610,000 g/mol were analyzed to generate Mark-Houink parameters for PEO in chloroform at 25°C, yielding $[\eta]=0.0707Mv^{0.676}$. Gel content was determined by extraction with chloroform from 120 mesh sieve cloth for 72 hours. The sample was dried under vacuum to constant weight, and gel content reported as the weight percent of insoluble polymer.

Alkyne grafting to cyclooctane. Stock solutions (5 ml) of cyclooctane containing the desired concentration of alkyne and DCP were charged to a series of 10 ml stainless steel pressure vessels and sealed under 1.5 MPa of N2. The vessels were immersed in an oil bath at 160 ºC under constant magnetic stirring. Alkyne conversions were quantified by 1H-NMR spectrum integration of the residual acetylenic resonance to the methylene group within EP and an aromatic resonance for PhCCH. Unreacted starting materials were removed by Kugelrohr distillation (0.03 bar, 110 ºC) and the residue was fractionated by semi-preparative, normal-phase HPLC using a Waters Model 400 instrument equipped with UV-Vis and refractive index detectors (5% ethyl acetate, 95% hexanes eluent, Supelcosil PLC-Si column).

Isolated products of cyclooctane-g-EP

Ethyl (2Z)-3-cyclooctylacrylate (1-Z). MS: required for $C_{13}H_{23}O_2^+$ *m/z* 211.1698; found *m/z* 211.1695. ^{1}H NMR [$CDCl_3$,δ]: 1.27 (t, 3H, -C**H**$_3$), 1.45-1.65 (14H, -(C**H**$_2$)$_7$-), 3.54 (m, 1H, -C**H**-CH=CH-), 4.15 (q, 2H, -OC**H**$_2$-), 5.58 (d, 1H, =C**H**-CO-), 6.08 (dd, 1H, -C**H**=CH-CO-).

Ethyl (2E)-3-cyclooctylacrylate (1-E). MS: required for $C_{13}H_{23}O_2^+$ *m/z* 211.1698; found *m/z* 211.1696. ^{1}H NMR [$CDCl_3$,δ]: 1.26 (t, 3H, -C**H**$_3$), 1.45-1.70 (14H, -(C**H**$_2$)$_7$-), 2.36 (m, 1H, -C**H**-CH=CH-), 4.15 (q, 2H, -OC**H**$_2$-), 5.72 (d, 1H, =C**H**-CO-), 6.93 (dd, 1H, -C**H**=CH-CO-).

Diethyl(2E,2E')-3,3'-cyclooctane-1,3-diylbisacrylate (E,E-2). MS: required for $C_{18}H_{28}O_4H^+$ *m/z* 309.41; found *m/z* 309.21. ^{1}H NMR [$CDCl_3$,δ]: 1.26 (t, 6H, -C**H**$_3$), 1.32-1.81 (10H, -(C**H**$_2$)$_5$-), 2.40 (m, 2H, -C**H**-CH=CH-), 2.51 (m, 2H, -C**H**$_2$-(CH-CH=CH)$_2$-), 4.16 (q, 4H, -OC**H**$_2$-), 5.73 (d, 2H, =C**H**-CO-), 6.89 (dd, 2H, -C**H**=CH-CO-).

Triethyl-1,3,5-benzenetricarboxylate (3). MS: required for $C_{15}H_{18}O_6^+$ *m/z* 294.1103; found *m/z* 294.1106. ^{1}H NMR [$CDCl_3$,δ]: 1.41 (t, 9H, -C**H**$_3$), 4.43 (q, 6H, -OC**H**$_2$-), 8.84 (s, 3H, aromatic). [20]

Isolated products of cyclooctane-g-PhCCH

1, 3, 5-Triphenylbenzene. MS: required for $C_{24}H_{18}^+$ *m/z* 306.1409; found *m/z* 306.1408. ^{1}H NMR [$CDCl_3$,δ]: 7.38 (t, 3H), 7.47 (t, 6H), 7.69 (d, 6H), 7.77 (s, 3H). [21]

1-Cyclooctyl-2, 4-diphenyl-1, 3-butadiene. MS: required for $C_{24}H_{27}^+$ *m/z* 315.2113; found *m/z* 315.2112. ^{1}H NMR [$CDCl_3$,δ]: 1.38-1.66 (m, 14H, - (C**H**$_2$)$_7$-), 2.59 (m, 1H, -CH$_2$-C**H**-CH$_2$-), 5.76 (d, 1H, -C**H**=C(Ph)-CH=CH-Ph), 6.33 (d, 1H, -CH=C(Ph)-C**H**=CH-Ph), 6.54 (d, 1H, -CH=C(Ph)-CH=C**H**-Ph).

Alkyne grafting to PEO and LLDPE. Polymer pellets (40 g) were tumble mixed

after the addition of DCP (0.08 g) as a chloroform solution. After evaporation of the solvent, the material was melt-mixed with the required amount of EP (0 g, 2 g) in the chamber of a Haake Polylab batch mixer (105ºC, 60 rpm, 5 min). Aliquots of the resulting masterbatch were reacted in the melt-sealed cavity of a parallel plate rheometer (Advanced Polymer Analyzer, Alpha Technologies) at 160ºC for 45 min. PE derivatives for structural characterization were purified by dissolving in hot toluene (PE) and precipitating from acetone, while PEO-derived products were similarly treated with methanol / chilled diethyl ether.

4.3 Results and Discussion

Radical-mediated polymer modifications generally yield low concentrations of inseparable products, making it difficult to characterize derivatives unambiguously. However, model compounds are amenable to chromatographic separation and detailed structural analysis, so our examination of alkyne grafting chemistry started with cyclooctane before progressing to poly(ethylene oxide) and polyethylene substrates. Concentration units of mmole per gram of hydrocarbon were used to maintain consistency between model and polymer systems.

Model Compound Studies. Ethyl propiolate (EP) addition has the potential to introduce polarity to a hydrocarbon while rendering it reactive toward conjugate addition, trans-esterification and trans-amidation reactions. Heating a cyclooctane solution containing 0.5 mmol/g EP to 160°C for 45 min under nitrogen had little

effect, but the addition of 7.4 μmol/g dicumyl peroxide (DCP) under these conditions converted 54% of the alkyne. Removal of residual monomer and unreacted cyclooctane gave the crude product whose ^{1}H-NMR spectrum is illustrated in Figure 4.1a.

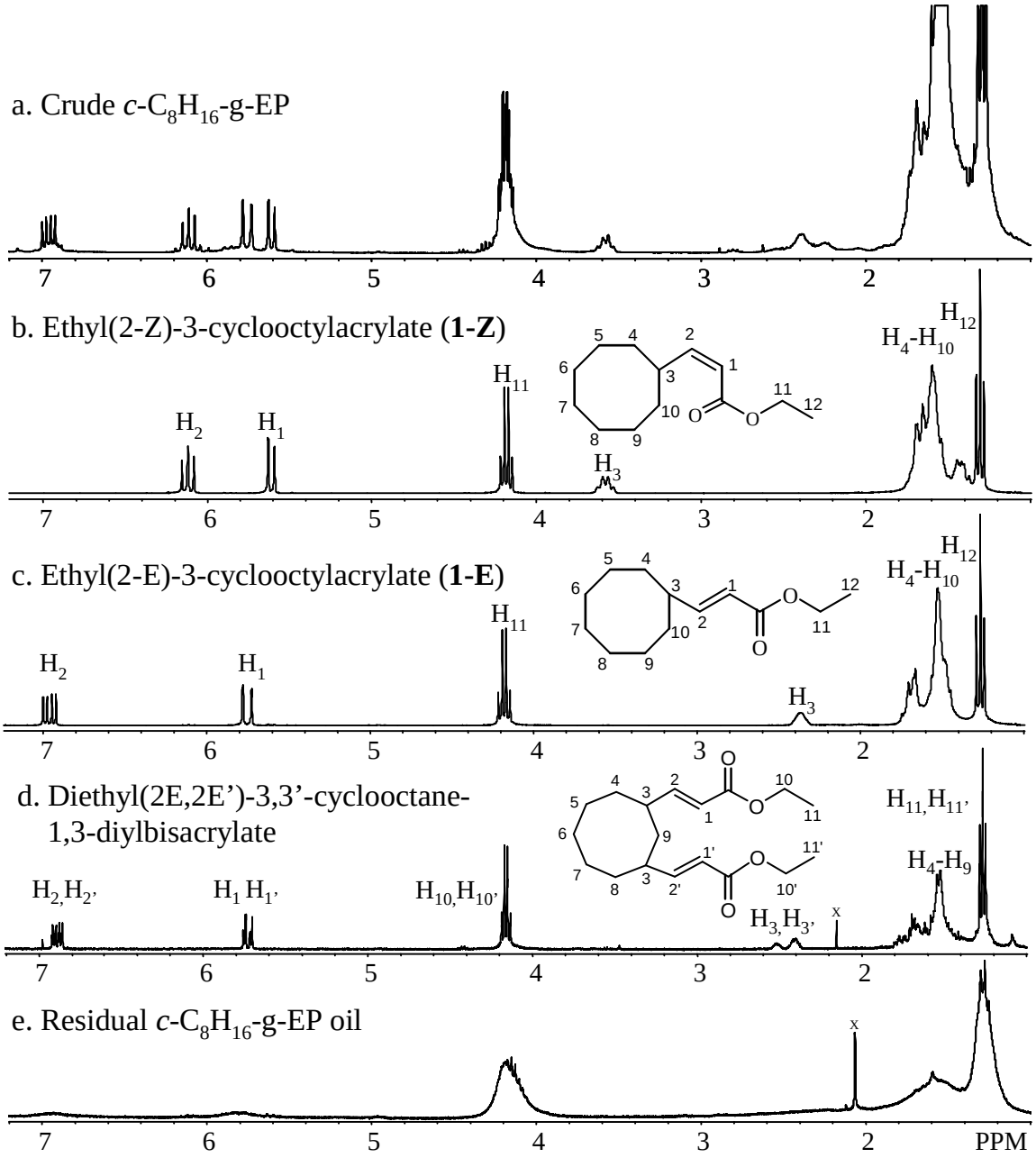

Figure 4.1. ^{1}H-NMR spectra of a. unfractionated *c*-C_8H_{16}-g-EP; b. ethyl (2Z)-3-cyclooctylacrylate (**1-Z**); c. ethyl (2E)-3-cyclooctylacrylate (**1-E**); d. diethyl (2E,2E')-3,3'-cyclooctane-1,3-diylbisacrylate; e. residual *c*-C_8H_{16}-g-EP oil.

HPLC fractionation of this crude product recovered several compounds (Scheme 4.2), with ethyl 3-cyclooctylacrylate (**1**) accounting for the majority of consumed monomer (Figures 4.1b,c). These simple addition products were produced in a 55:45 ratio of E:Z isomers, which is on the order of that reported for cyclohexane addition to methyl propiolate at a comparable temperature. [11, 22] Reports of radical addition to alkynes focus solely on the yield of 1:1 adducts, with little or no attention paid to byproducts. However, polymer derivatives contain every form of bound alkyne, and can rarely be fractionated on the basis of chemical composition. Therefore, complete characterization of an alkyne-modified polymer requires knowledge of the full range of reaction products, leading us to extend our analysis toward more complex EP-derived compounds.

Scheme 4. 2: Isolable compounds of *c*-C_8H_{16}-g-EP

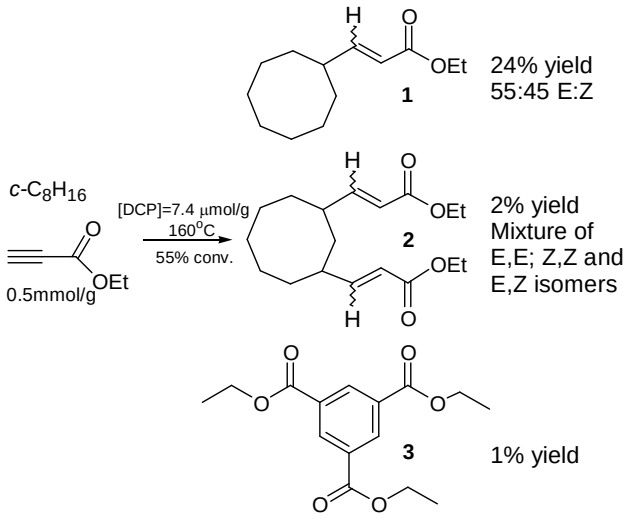

A small amount of 2:1 EP:cyclooctane adducts (**2**, Scheme 4.2) was recoverable by HPLC. These compounds are the product of a 1,5-intramolecular hydrogen atom

abstraction by an intermediate vinyl radical, followed by EP addition to the resulting secondary alkyl radical. These radical translocations are well-established for vinyl radicals, [16] and are known to affect polyolefin oxidations [23] as well as graft modifications involving maleic anhydride [24] and vinylsilanes. [25] In the context of alkyne addition, this process generates a mixture of steroisomers and E,Z-configurational isomers, one of which, diethyl (2E,2E')-3,3'-cyclooctane-1,3-diylbisacrylate, was characterized as a representative example (Figure 4.1d).

The appearance of triethyl-1,3,5-benzenetricarboxylate (**3**) crystals, and smaller amounts of the 1,2,4-trisubstituted isomer, was unexpected. Transition metal catalyzed [26] and mediated [27] alkyne cyclotrimerizations are well known, but clearly documented examples of radical-mediated processes at moderate temperatures are comparatively rare. [28] Control experiments involving the heating of ethylpropiolate and cyclooctane in the absence of peroxide produced no aromatic products. Therefore, we propose a radical mechanism akin to that suggested by Drew and Gordon, [18] wherein repeated EP addition generates an oligomeric vinyl radical, whose cyclization eliminates an alkyl (or vinyl) radical to give a tri-substituted aromatic.

While triethyl-1,3,5-benzenetricarboxylate was easily isolated, the remaining oligomerization products constituted an intractable orange oil that amounted to 45%

of converted alkyne. Based upon ^{1}H-NMR spectrum integration (Figure 4.1e), this complex mixture had an overall composition of 3.8:1 EP:cyclooctane, which is consistent with oligomeric compounds of variable composition. Poor spectrum resolution is indicative of the mixture's complexity, and resonances in the downfield olefinic region are not as abundant as might be expected. This is likely due to the reactivity of conjugated polyenes, whose radical attack is expected to contribute a wide range of ill-defined products. [7]

We noted that cyclooctane produced reasonable yields of ethyl (2-E,Z)-3-alkylacrylates (Scheme 4.2), but analogous n-octane reactions generated a complex oil at the expense of simple 1:1 addition products. The homolytic C-H bond dissociation energy of cyclooctane is considerably less than that found in other hydrocarbons (i.e. 389.6 kJ/mol for C_8H_{15}-H versus 400.2 kJ/mol for C_6H_{11}-H), [29] which makes it more susceptible to radical oxidation, [30] and heightens its rate of hydrogen atom donation to alkoxyl [31] and alkyl [32] radicals. The importance of hydrogen transfer to alkyne additions has been demonstrated by Kopping et al., who exploited the reactivity of $(Me_3Si)_3SiH$ to carry out radical-mediated hydrosilylations that are not accessible to standard trialkylsilanes. [12] In the present context, differences in the reactivity of cyclooctane and n-octane as hydrogen donators shifted products from simple mono-adducts toward polyene oligomers.

Having defined the main products of EP activation, our attention turned to the sensitivity of cyclooctane + EP conversions to alkyne and initiator concentrations.

The data plotted in Figure 4.2a show that irrespective of the initial monomer loading, quantitative EP conversions could be achieved given a sufficient amount of DCP. Evidence of the reaction's chain character is provided by estimates of peroxide yields that we define as the moles of converted alkyne per mole of initiator-derived radicals. Since alkyne concentrations decline during a batch reaction, and the fraction of peroxide-derived radicals that contribute directly to EP consumption are unknown, peroxide yields represent minimum values of the kinetic chain length. Nevertheless, values as high as 33 mol/mol were recorded at low EP conversions – clear evidence of a radical chain process of alkyne addition.

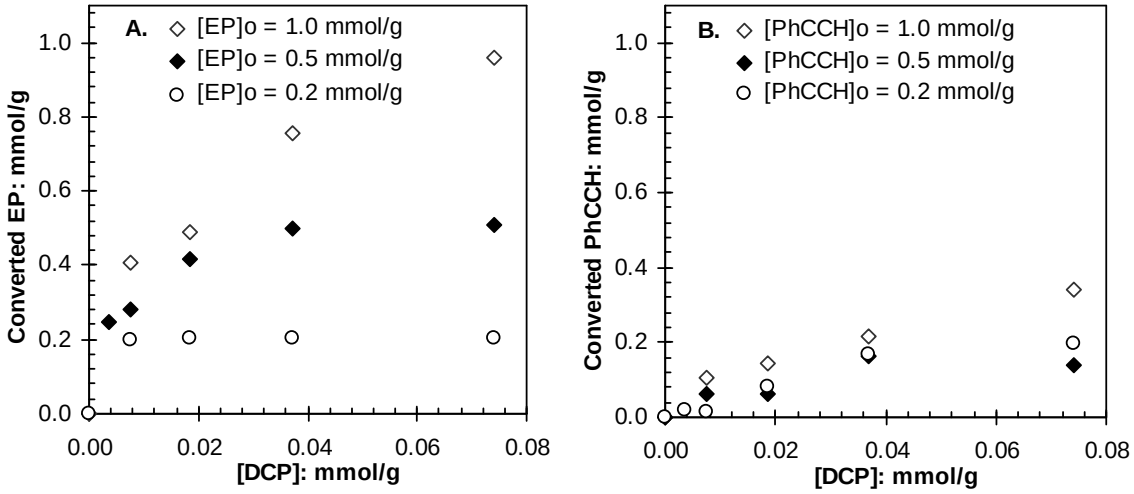

Figure 4.2: Converted alkyne versus DCP concentration; a. Ethyl propiolate; b. Phenyl acetylene; (cyclooctane, T=160°C, 45 min).

The data presented in Figure 4.2a also show that reaction yields respond to EP availability. Polymerizations are expected to be sensitive to monomer concentrations, but such a simple relationship is not inherent for grafting processes

that involve radical addition and hydrogen atom transfer (Scheme 4.1). A first-order dependence of grafting rates on monomer concentration is observed when addition is rate limiting, [33] while a zero-order dependence is seen when hydrogen donation is relatively slow. [34] That reaction yields varied with EP concentration suggests that hydrogen atom donation by cyclooctane to intermediate vinyl radicals is not rate-controlling. The relationship between a polymer's hydrogen atom donation properties and its alkyne grafting chemistry are explored following a brief examination of the phenylacetylene system.

Phenylacetylene. Unlike the EP additions, peroxide yields of cyclooctane + PhCCH reactions did not exceed 7.3 mol/mol, and alkyne conversions did not respond strongly to changes in monomer concentration (Figure 4.2b). We noted above that modifier loadings have little bearing on graft propagation rates when hydrogen atom transfer is much slower than alkyl radical addition to monomer (k_{tr}[R-H] < k_{add}[PhCCH]; Scheme I). The atom abstraction efficiency of RHC=C(·)Ph vinyl radicals is known to be quite poor, [35] with stabilization provided by an α-Ph substituent likely contributing to this inefficiency.[36]

PhCCH-derived products were consistent with those derived from a propagation sequence that is limited by hydrogen atom transfer. Only 1,3,5-triphenyl benzene was produced in isolable quantities (1-3%), with trace amounts of single-graft adducts analogous to **1** evident in ^{1}H-NMR spectra of crude reaction mixtures. Residual

products comprised an oil from which only one compound, 1-cyclooctyl-2,4-diphenyl-1,3-butadiene, was isolated. This compound is not important in terms of reaction yield, but it is a significant example of a polyene generated by cyclooctyl radical attack on an alkyne. As such, it reinforces our assertion that oligomerization can contribute to alkyne consumption, especially when vinyl radical trapping by hydrogen transfer is relatively slow.

Polymer Modifications. The development of a modification process must be concerned with the composition of the new material (structure and amount of grafted monomer) and any molecular weight changes (crosslinking and/or fragmentation) that accompany polymer functionalization. Poly(ethylene oxide) (PEO) and polyethylene (PE) were of particular interest, since both materials generate secondary alkyl macroradicals without producing regioisomers, and yet they differ substantially in terms of C-H bond dissociation energy. Consider the reported values for H-2-tetrahydrofuranyl (385 kJ/mol) versus H-cyclohexyl (400 kJ/mol). [37] This difference is larger than that encountered in the cyclooctane/n-octane reactions described above, and suggests that PEO will generate higher alkyne graft yields and simpler product distributions than PE.

^{1}H-NMR analysis of functionalized polymer derivatives supports this assertion (Figure 4.3). The downfield region of the PEO-g-EP spectrum shows clear evidence of the ethyl(2-E,Z)-3-alkylacrylates found in the cyclooctane system, as well as smaller amounts of oligomeric byproducts. On the other hand, the spectrum of

PE-g-EP shows broad resonances in the heteroatom and olefinic regions that are consistent with the polyene mixtures found in n-octane-g-EP and, to a lesser degree, within cyclooctane-g-EP.

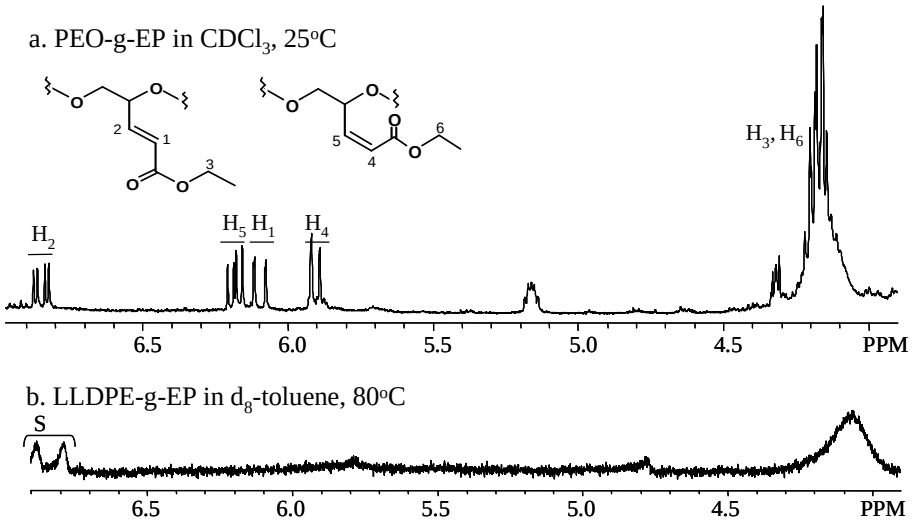

Figure 4. 3: Downfield ^{1}H-NMR spectra of purified polymer derivatives, a. PEO-g-EP; b. PE-g-EP.

PE and PEO modifications differ not only in terms of product structure, but in terms of kinetic chain length (Table 4.1). The PE-g-EP system generated a peroxide yield of 3.4 mol/mol, while an equivalent PEO-g-EP reaction produced a value of 12.2 mol/mol. That a polymer modification can meet an alkyne conversion target using less initiator has obvious implications for reaction economy. However, selectivity for polymer functionalization versus molecular weight alteration is equally important. Given that macro-radical combination and fragmentation yields are tied directly to initiator loadings, grafting processes that provide superior kinetic chain lengths allow monomer conversion targets to be reached while minimizing the yield of undesirable side-reactions. In general, PE modifications build molecular weight through

macro-radical combination, [3] and good peroxide yields are needed to achieve appreciable graft contents without incurring excessive cross-linking. The low molecular weight of our starting PE material prevented its PE-g-EP derivative from reaching the gel point, but similar experiments with high molecular weight commercial materials gave only thermoset products.

Table 4. 1 Yields of PE and PEO additions to Ethyl Propiolate[a]

Polymer	[DCP] μmol/g	[EP] mmol/g	Grafted EP mmol/g	Peroxide Yield mol/mol	[η] dl/g	M_v kg/mol
PE	7.4	0.51	0.05	3.4	---	---
PEO	---	---	---	---	15.6	132
PEO	3.7	0.51	0.11	15.4	13.0	68
PEO	7.4	0.51	0.18	12.2	12.5	65
PEO	18.5	0.51	0.29	7.8	14.3	78
PEO	37.4	0.51	---	---	---	37% gel
PEO	3.7	0.00	---	---	13.5	69
PEO	7.4	0.00	---	---	11.0	53
PEO	18.5	0.00	---	---	8.8	38
PEO	37.4	0.00	---	---	---	2% gel

a. T=160°C; 45 min. The gel content measurement are of the same procedure as described in page 18, but toluene was changed to chloroform and acetone was changed to diethyl ether.

Molecular weight changes observed for PEO modifications are more complex than those seen in corresponding PE processes, owing to the susceptibility of polyethers toward macro-radical scission. [38] It is known that low peroxide loadings (less than 37.4 μmol/g / 1 wt% DCP) reduce the number average molecular weight and polydispersity index of PEO. [39] On the other hand, DCP concentrations above 3 wt% can lead to PEO gelation, as macro-radical lifetimes decline to the point that β-scission is suppressed relative to radical-radical combination. [40] The molecular

weight data presented in Table 4.1 are consistent with these published findings. In the absence of alkyne monomer, the molecular weight of our PEO fell from 132 kg/mol to 38 kg/mol when the polymer was heated with 18.5 μmol/g of DCP at 160°C, while a much higher peroxide loading of 37.4 μmol/g produced a small amount of chloroform-insoluble gel.

Very different behaviour was observed when a significant amount of EP was converted to pendant PEO grafts. The data listed in Table 4.1 show that chain scission was the dominant molecular weight altering reaction when peroxide loadings failed to bring alkyne conversions beyond 35%. However, raising the initiator concentration to 18.5 μmol/g provided a monomer conversion of 56% and a molecular weight that was **greater** than observed at lower DCP concentrations. Doubling the initiator loading to 37.4 μmole/g DCP yielded an extensively cross-linked product with a chloroform-insoluble gel content of 37%.

These measurements show that EP can serve as a di-functional monomer in the manner of multifunctional allyl and acrylate coagents, [41] with alkyne addition producing unsaturated grafts that can be activated by macro-radical addition and/or allylic hydrogen abstraction for the purposes of cross-linking. According to this model, ethyl (2-E, Z)-3-alkylacrylate functionality and EP-derived polyene oligomers are reactive intermediates in a PEO cross-linking process. To counter the effects of macro-radical fragmentation on molecular weight, these intermediates must be

generated in sufficient quantity. It follows, therefore, that the extent of PEO-g-EP cross-linking should vary with alkyne conversion in the observed manner. Support for this theory comes from the reported ability of acetylene to boost the cross-link density of peroxide-cured LDPE. [5] This would require acetylene addition to generate pendant vinyl and/or polyene functionality, and activate these groups for the purposes of cross-linking. In the context of EP additions, alkyne graft yields to PE are relatively low and the addition products are more highly substituted than anticipated acetylene analogues. Therefore, expectations for alkyne-assisted cross-linking should be tempered by knowledge of the amenability of a polymer toward EP addition.

4.4 Conclusions.

Free-radical addition of poly (ethylene oxide) to EP under high-temperature, solvent-free conditions provides good yields of ethyl (2-E, Z)-3-alkylacrylates. However, alkyne graft yields and structures are sensitive to the polymer's reactivity toward hydrogen atom transfer, with polyether modifications providing higher peroxide yields and simpler reaction products than analogous polyethylene derivatizations. Where the trapping of intermediate vinyl radicals is relatively inefficient, alkyne oligomerization yields a complex mixture of polyenes and cylcotrimerized aromatics. The selectivity of polyether modifications for alkyne addition versus molecular weight variation varies with EP conversion, with alkylacrylate functionality serving as a reactive intermediate in the polymer

cross-linking process.

4.5 References and notes.

1. This chapter has been published as: Wu, W. and Parent, J.S., *J. Polym. Sci., Part A: Polym Chem.*, **2008**, *46*, 7386-7394.
2. Russell, K. E. *Prog Polym Sci.* **2002**, *27*, 1007-1038
3. Moad, G. *Prog. Polym. Sci.* **1999**, *24*, 81-142.
4. Parent, J. S.; Tripp, M.; Dupont *J. Polym Eng Sci.* **2003**, *43*, 234-242.
5. Wong, W.K.; Varrall, D.C. *Polymer*, **1994**, *35*, 5447-5452.
6. Mitsui, H.; Hosoi, F.; Kagiya, T. *Polym J.* **1974**, *6*, 20-26.
7. Amiel, Y. In The *Chemistry of Functional Groups, Supplement*, C, S. Patai and Z. Rappoport, Eds. Wiley, **1983**, Chapter 10.
8. Julia, M. In The *Chemistry of Acetylenes*, H. G. Viehe, Ed. Marcel Dekker, **1969**, 335-354.
9. Renaud, P.; Beaufils, F.; Feray, L.; Schenk, K. *Angew. Chem.* Int Ed **2003**, *42*, 4230-4233.
10. Curran, D.P.; Porter, N.A.; Geise, B. In *Stereochemistry of Radical Reactions*, VCH, Weinheim, **1995**.
11. Cywinski, N.F.; Hepp, H.J. *J. Org. Chem.***1965**, *30*, 3814-3817.
12. Metzger, J.O.; Blumenstein, M. *Chem Be.* **1993**, *126*, 2493-2499.
13. Kopping, B.; Chatgilialoglu, C.; Zender, M.; Giese, B. *J. Org. Chem.* **1992**, *57*, 3994-4000.

14. Giese, B.; Lachhein, S. *Angew Chem* Int Ed Engl, **1982**, *21*, 768.

15. Fischer, H.; Radom, L. *Angew Chem* Int Ed Engl, **2001**, *40*, 1340-1371.

16. Gaizith, M.; Szwarc, M. *J. Amer. Chem. Soc.* **1957**, *79*, 3339-3343.

17. a. Curran, D. P.; Dooseop, K.; Hong, T. L.; Shen, W. *J. Amer. Chem. Soc.* **1988**, *110*, 5900-5902. b. Curran, D. P.; Shen, W. *J. Amer. Chem. Soc.* **1993**, *115*, 6051-6059.

18. Drew, C. M.; Gordon, A.S. *J. Chem. Phys.* **1959**, *31*, 1417-1481.

19. Huggins, M. L. *J. Amer. Chem. Soc.* **1942**, *64*, 2716-2718.

20. Nielsen, A. T.; Christian, S. L.; Moore, D. W.; Gilardi, R. D.; George, C. F. *J. Org. Chem.* **1987**, *52*, 1656-62.

21. Kumar, V. G., Shoba, T. S., Rao, K. V. C., *Tetrahedron Lett*, **1985**, *26*, 6245-6248.

22. Giese, B.; Gonzalez-Gomez, J. A.; Lachhein, S.; Metzger, J. O., *Angew. Chem.* Int Ed **1987**, *26*, 479-480.

23. Rust, F.F. *J. Amer. Chem. Soc.*, **1957**, *79*, 4000-4003.

24. Russell, K. E.; Kelusky, E. C. *J. Polym. Sci., Part A: Polym. Chem.* **1988**, *26*, 2273-2280.

25. Forsyth, J.C.; Baker, W.E.; Russell, K. E.; Whitney, R.A., *J. Polym. Sci. Part A: Polym. Chem.*, **1997**, *35*, 3517-3525.

26. a. Kotha, S.; Brahmachary, E.; Lahiri, K. *Eur. J. Org. Chem.* **2005**, *22*, 4741-4767. b. Saito, S.; Yamamoto, Y., *Chem. Rev.*, **2000**, *100*, 2901-2915.

27. Yamamoto, Y. *Current. Org. Chem.* **2005**, *9*, 503-519.

28. a. Zhu, Z.; Wang, J.; Zhang, Z.; Xiang, X.; Zhou, X. *Organometallics*, **2007**, *26*, 2499-2500. b. Yang, J.; Verkade, J. G. *Organometallics*, **2000**, *19*, 893-900. c. Yang, J. and Verkade, J. G. *J. Amer. Chem. Soc.*, **1998**, *120*, 6834-6835.
29. Fujisaki, N.; Ruf, A.; Gaumann T. *J. Amer. Chem. Soc.* **1985**, *107*, 1605-1610.
30. Cook, G. K.; Mayer, J. M., *J. Amer. Chem. Soc.* **1995**, *117*, 7139-7156.
31. Bunce, N. J.; Hadley, M., *J. Org. Chem.* **1974**, *39*, 2271-2276.
32. a. Alfassi, Z. B.; Feldman, L., *Int. J. Chem. Kinet.* **1981**, *13*, 517-526. b. Parent, J. S.; Wu, W.; Sengupta, S.S.; Jackson, P., *Eur. Polym. J.* **2006**, *42*, 971-980.
33. Parent, J. S.; Parodi, R.; Wu, W., *Polym. Eng. Sci.*, **2006**, *46*, 1754-1761.
34. Sipos, A.; McCarthy, J.; Russell, K. *J. Polym. Sci. Part A: Polym. Chem.* **1989**, 27, 3353-3362.
35. Kharasch, M. S.; Jerome, J. J.; Urry, W. H. *J. Org. Chem.* **1950**, *15*, 966-972.
36. Branchi, B.; Galli, C.; Gentili, P. *Eur. J. Org. Chem.*, **2002**, *16*, 2844-2854.
37. McMillan, D. E.; Golden, P. M. *Ann. Rev. Phys. Chem.* **1982**, *33*, 493-532.
38. Bortel, E.; Lamot, R. *Makromolekulare Chemie*, **1977**, *178*, 2617-28.
39. Wang, J. H.; Schertz, D. M.; Golden, B. A. WO 99/33899, **1999**.
40. a. Row, P. D.; Thomas, D. K. *J. Appl. Polym. Sci.*, **1963**, *7*, 461-468. b. Emami, S. H.; Salovey, R.; Hogen-Esch, T. E., *J. Polym. Sci. Part A: Polym. Chem.*, **2002**, *40*, 3021-3026.
41. Yakabe, Y.; Sudoh, Y.; Takahata, Y., *J. Chromatog.*, **1991**, *558*, 323-327.

Chapter 5 A Grafting/oligomerization Variation of Precipitation Polymerization.

5.1 Introduction.

In the course of studying reactive extrusion approaches to introduce long-chain branching to polypropylene, Parent and coworkers discovered a small amount of sub-micron particles dispersed within the products.[1] These reactions involved peroxide-initiated grafting of triallyl trimesate (TAM) under solvent free conditions, with the intention of exploiting macro-radical scission and coagent-assisted cross-linking to transform a linear starting material into a branched derivative. The appearance of TAM-rich particles (Figure 5.1) is consistent with a precipitation polymerization process in which the activation of a trifunctional coagent results in phase-instability, and cross-linking of a concentrated adduct phase to give solid microspheres.

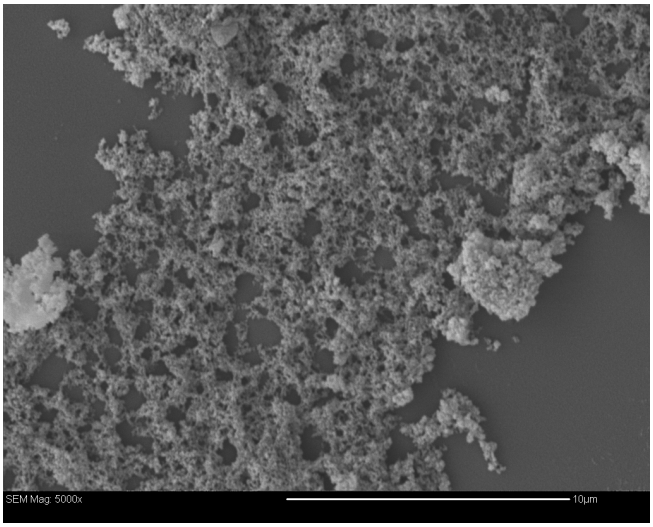

Figure 5.1 SEM photo of particles separated from grafted PP with TAM as coagent. (5000x)

There is a substantial body of literature on the production of crosslinked microspheres through precipitation [2,3] dispersion [4, 5] polymerizations of mono- and di-functional acrylates, [6, 7] styrenics [8, 9, 10] and their mixtures. [11, 12, 13] The discovery of hydrocarbon+triallyl coagent derived particles motivated further research into a new variation of the precipitation approach, wherein intermolecular C-H bond addition to an olefin (Scheme 5.1) contributes to molecular weight growth. This adaptation may widen the scope of particle syntheses by incorporating functional molecules that do not contain polymerizable C=C bonds.

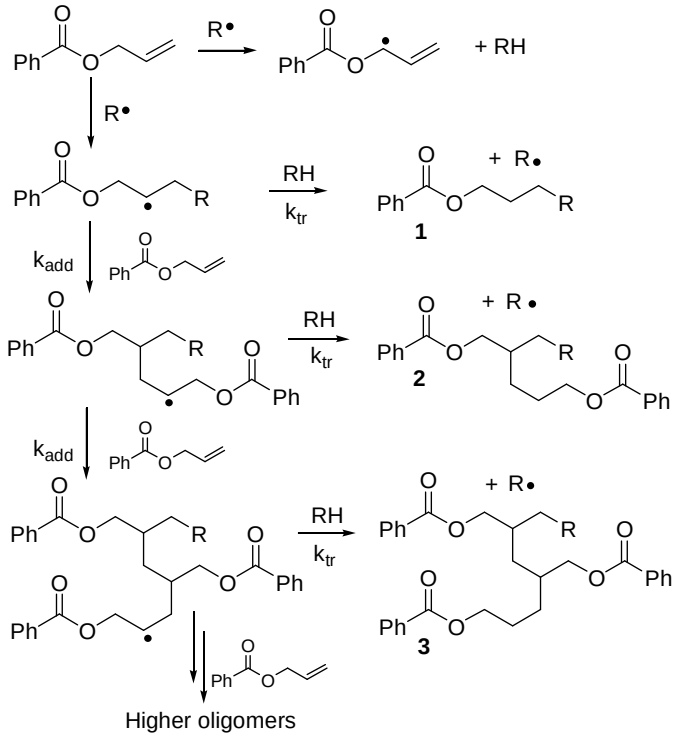

Scheme 5.1 Expected reactions of allyl benzoate in hydrocarbon in the presence of radicals.

The radical-mediated addition of aliphatic hydrocarbons to olefins is a chain sequence of alkyl radical addition and hydrogen atom abstraction by the resulting adduct radical from the hydrocarbon. [14] Direct hydrogen transfer from the hydrocarbon presents

challenges with respect to the rate of adduct radical trapping, given the relative strength of C-H bonds. These limitations have been mitigated to some extent in peroxide-initiated polyolefin functionalizations that by necessity are conducted at melt temperatures that are sufficiently high to yield reasonable kinetic chain lengths. [15, 16] In the present context, R-H addition and oligomerization reactions of a tri-functional monomer are intended to build hydrocarbon+monomer adducts to concentrations above their solubility limit. Reaction-induced phase separation is to give a dispersed phase of concentrated adducts, whose continued oligomerization and C-H bond addition should generate crosslinked particles.

By activating saturated hydrocarbons, this new approach provides additional degrees of freedom for tailoring particle composition. However, success requires careful consideration of alkene reactivity. If the hydrocarbon is to be incorporated into a particle, reactivity in a dilute monomer solution must allow for C-H bond addition, meaning that $k_{tr}[RH] \approx k_{add}[RCH{=}CH_2]$ (Scheme 1). Such a balance is difficult to achieve with acrylic and styrenic monomers, but allylic systems are much less reactive with respect to radical addition, [17, 18] and the resulting adduct radical is of similar energy, polarity and philicity to hydrocarbon-derived alkyl radicals. Hence, high-temperature reactions of allyl monomers may provide the necessary balance between hydrogen atom transfer and repeated monomer addition. [19]

The simplest variation of this synthesis uses a tri-allyl compound, a saturated

hydrocarbon, and an organic peroxide initiator. Precipitation and dispersion polymerizations exploit solvent mixtures that cannot solvate oligomeric intermediates due to unfavourable polymer-solvent interactions (enthalpic contributions to excess Gibbs energy) and/or due to differences in molecular weight and architecture (entropic contributions). [20] In the present context, solvent selection is limited to compounds that are less efficient hydrogen atom donors than the saturated substrate that is to be incorporated into the particle. Therefore, if aliphatic hydrocarbons such as cyclooctane are targeted, solvents should be restricted to non-alkylated aromatics, or avoided altogether.

A final reaction requirement centres on the reactivity of hydrocarbon-monomer adducts within a concentrated, dispersed droplet phase. If crosslinking to the point of mechanical integrity is desired, then adduct oligomerization is a preferred mode of molecular weight growth. This requires $k_{add}[RCH=CH_2]$ within adduct droplets to support a degree of polymerization that renders a stable particle (Scheme 1). Although radical reactions of allyl monomers are inhibited by degradative chain transfer through allylic hydrogen abstraction, [21, 22] the kinetic chain lengths reported for allylic ester polymerizations should be sufficient to render a crosslinked entity from a concentrated adduct phase. [23]

This chapter describes studies of this variation of precipitation polymerization. The intrinsic reactivity of allylic esters is examined in the context of C-H addition and

oligomerization by analysis of allyl benzoate reaction products, and these results are extended to the triallyl trimesate (TAM) system to generate cross-linked microspheres.

5.2 Experimental

Materials.

Allyl benzoate (AB, 99%, TCI), triallyl trimesate (TAM, 99%, Monomer Polymer Inc), dicumyl peroxide (DCP, 98%, Sigma-Aldrich), L231 and cyclooctane (CyOc, 99%, Sigma-Aldrich) were used as received.

Instrumentation and Analysis.

Semi-preparative fractionation of model compounds was accomplished by high pressure liquid chromatography (HPLC) with a Waters Model 400 instrument equipped with a normal-phase Supelcosil PLC-Si column and differential refractive index as well as UV-Vis detectors. NMR spectra were recorded with a Bruker AM-600 spectrometer (600.17 MHz ^{1}H, 150.92 MHz ^{13}C) in $CDCl_3$, with chemical shifts reported relative to tetramethylsilane.

5.2.1 Cyclooctane-g-allyl benzoate.

Cyclooctane (3g, 26 mmole), the desired amount of allyl benzoate and DCP (0.009g, 0.3wt% of cyclooctane) were sealed in a pressure tube and heated to 170º C for 20 min under a nitrogen atmosphere. Unconsumed reagents were removed by Kugelrohr distillation (0.08mm Hg, 80°C) to yield a highly viscous liquid, CyOc-g-AB.

Quantitative integration of ^{1}H NMR spectra revealed 40% of allyl groups were consumed. Fractionation by normal-phase HPLC (5% ethyl acetate, 95% hexanes eluent) produced three components; the column was then flushed with 15% ethylacetate-85%hexane to collect all injected samples. All four fractions were collected and subjected to NMR analysis.

5.2.2 Cyclooctane-g-triallyl trimesate.

Cyclooctane (3g, 26 mmole) and the desired amount of triallyl trimesate (0.03g-0.15g, 0.09 mmole-0.45 mmole) were sealed in a stainless steel autoclave, pressurized to 200 psi with N_2 and heated to the desired reaction temperature (170°C, 145°C) under continuous agitation. A cyclooctane solution containing the desired concentration of DCP (0.003g-0.015g, 0.011 mmole-0.055 mmole) was injected under pressure, and stirring was continued for five initiator half-lives.

The autoclave was cooled to room temperature and the contents filtered to isolate a liquid containing residual TAM and cyclooctane-soluble TAM-derived products, and solids containing cross-linked particles and cyclooctane-insoluble TAM-derived products (Scheme 5.2). The liquid fraction was analyzed for TAM content by gas chromatography. An aliquot of this liquid isolated from residual cyclooctane by Kugelrohr distillation, and the allyl and hydrocarbon content of the graft-modified products determined by ^{1}H-NMR spectroscopy.

The cyclooctane-insoluble reaction solids were washed with hexanes, dried under vacuum and weighed to record mass-based yields. The resulting material was extracted with xylenes to separate soluble TAM-derived products from cross-linked particles. The soluble material was analyzed by ^{1}H-NMR for allyl and hydrocarbon content, while the composition of crosslinked solids was determined by elemental analysis for carbon, hydrogen and oxygen content to give the relative proportions of cyclooctane and TAM. Further analyses included scanning electron microscopy of gold-coated samples, powder X-ray diffraction and differential scanning calorimetry.

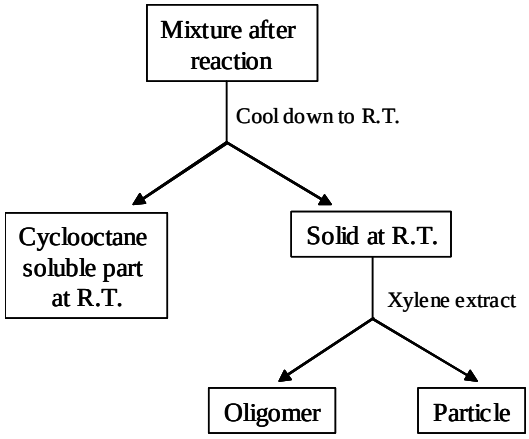

Scheme 5. 2 Treatment of the products after TAM particle synthesis.

Composition and yield data are reported for cross-linked solids, and for soluble TAM-derived products recovered from the cyclooctane-rich reaction mixture and by xylenes extraction of cyclooctane-insoluble material. Particle syntheses were also performed in a glass pressure tube to gain visual information on the process under static and agitated conditions. These reaction products were not analyzed for composition, but the cross-linked solids were examined by SEM to assess product morphology.

5.3 Results.

5.3.1 Allylic ester reactivity.

The peroxide-initiated addition of cyclooctane to allyl benzoate (AB) generates soluble products whose abundance reflects the nature of allylic ester activation in the absence of phase-partitioning effects. NMR spectra (Figure 5.2) of fractionated cyclooctane-g-AB products revealed mono-graft (**1**, Scheme 5.1), dimer (**2**), trimer (**3**) and oligomer residue.

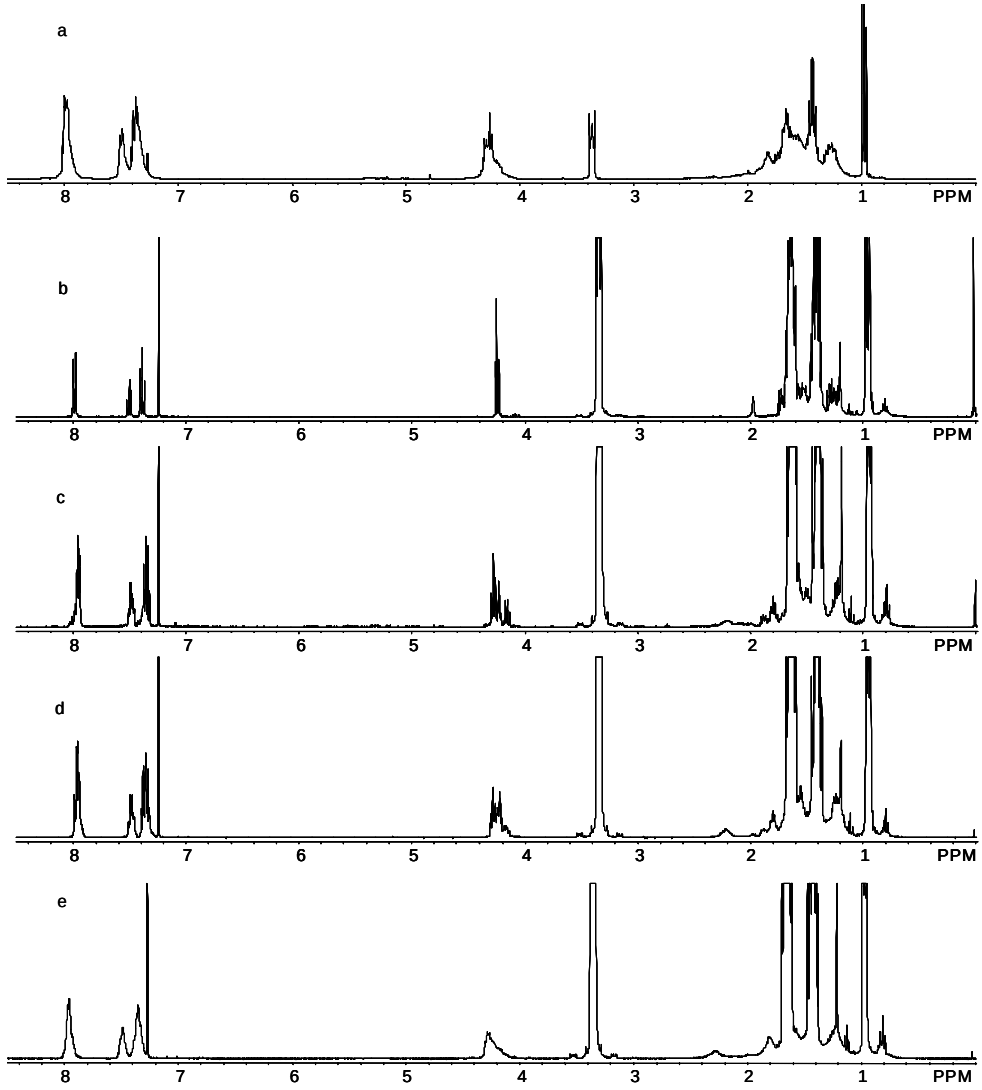

Figure 5.2. NMR spectra of isolated compounds from cyclooctane-allylbenzoate reaction (with TBAB as internal standard). a. Crude, b. mono-adduct product (1); c. di-adduct product (2); d. tri-adduct product (3); e. Oligomeric residue.

The yield data listed in Table 5.1 reveal the influence of AB concentration on grafting yields, as well as the relative rates of adduct radical trapping through hydrogen transfer and oligomerization. Overall AB conversions ranged from 30% to 60%, with peroxide yields responding positively to increased monomer availability. As mentioned in the previous chapters, peroxide yield is defined as the moles of monomer (AB in this case) consumed per mole of initiator-derived radicals. The values listed in Table 5.1 are modest in comparison to those seen for analogous maleation and vinylsilane additions, and are likely to be impacted negatively by allylic hydrogen atom abstraction, whose degradative effect on allyl monomer polymerizations is well established.

Table 5.1 Products distribution of cyclooctane grafting onto Allyl Benzoate.

CyOc:AB Molar Ratio	AB Conversion (mole %)	Peroxide Yield (mol/mol)	Product Molar Ratio **1** : **2** : **3**	Residual AB Products (mole % of converted AB)
100:1	60	3	86 : 12 : 02	8
50:1	55	5	76 : 19 : 05	3
25:1	40	7	63 : 26 : 11	9
5:1	30	22	43 : 30 : 27	52

0.3 wt% DCP; 170°C

Products generated at low AB loadings are dominated by mono-adduct (**1**), dimer (**2**), and trimer (**3**), with residual material accounting for less than 10 % of converted AB. At a 100:1 loading of cyclooctane:AB, the observed 86:12:2 distribution of **1**:**2**:**3** is clear evidence that grafting AB onto cyclooctane is preferred to repeated C=C

addition. This condition holds for a 50:1 solution, but fails when cyclooctane:AB ratios are brought to 5:1. At this point, oligomerization dominates to the extent that ill-defined telomers constitute 52% of converted AB. This shift from grafting-intensive to oligomerization-intensive with changing allyl ester concentration is necessary for a particle synthesis wherein R-H addition is used to build insoluble coagent adducts, whose phase separation is to be followed by residual C=C group oligomerization to yield cross-linked particles.

5.3.2 Triallyl trimesate Reactivity

Based on the principles described above, the symmetric trifunctional monomer triallyl trimesate (TAM) is expected to provide the requisite balance of C-H bond addition and oligomerization without incurring complications due to cyclization. Note, however, that the monomer concentrations needed to produce microspheres favour oligomerization to give complex product mixtures. As a result, our analysis was limited to determinations of the average number of cyclooctyl and allyl groups per molecule of converted TAM (Table 5.2).

Table 5. 2 Particle production under different experiment conditions.

					Xylene-Soluble Products			Insoluble Solid Products		
Expt.	C_8H_{16}:TAM Molar Ratio	[DCP] μmole/g	Temp ^oC	TAM Conversion %	TAM Yield[a] mole %	C_8H_{16}:TAM Molar Ratio	Allyl:TAM Molar Ratio	TAM Yield[a] %	Overall Yield[b] wt%	C_8H_{16}:TAM Molar ratio
A	100 : 1	7.4	170	76	100	1.7 : 1	1.0:1	0	0	---
B	56 : 1	7.4	170	73	99+	1.5 : 1	0.9:1	<1	trace	0.4 : 1
C	56 : 1	14.8	170	88	99+	1.9：1	0.6:1	<1	trace	0.5 : 1
D	56 : 1	14.8	145	>99	69	1.7：1	0.5:1	23	1.5	0.8 : 1
E	56 : 1	37.0	145	>99	74	1.9：1	0.4:1	19	1.2	0.8 : 1
F	56 : 1	74.0	145	>99	76	2.5：1	0.3:1	18	1.1	0.8 : 1

a. Mole percent of converted TAM in this product

b. Weight percent of total C_8H_{16}+TAM mixture in crosslinked solids

Dilute solutions of TAM in cyclooctane did not produce a crosslinked solid phase, as a 100:1 C_8H_{16}:TAM solution remained clear while 7.4 μmole/g of DCP was decomposed at 170°C. It did, however, become cloudy on cooling to room temperature to give a cyclooctane-rich solution, and an oil comprised of cyclooctane+TAM adducts. Adding xylenes re-established a homogeneous condition, leaving no solid or oil residue behind. Of the TAM charged to the reaction, 24% was unreacted, with the remaining 76% of converted monomer having an average of 1.7 mol cyclooctane and 1.0 mol of allyl functionality per mol of aromatic ester (Table 5.2, Expt. A). This average composition is ideal from the standpoint of hydrocarbon-rich particle formation, since TAM is converted to adducts that can oligomerize within a dispersed phase. However, reaction-induced phase instability was not observed under these conditions.

Three independent variables can be adjusted in an attempt to induce phase instability – initiator loading, monomer concentration, and reaction temperature. Although peroxide concentration can affect allyl group conversion, there was little scope to improve on Expt A, Table 5.2. On the other hand, increased monomer concentrations are expected to raise the concentration of hydrocarbon+monomer adducts while promoting oligomerization. Given that TAM-derived oligomers (dimers, trimers, etc.) are expected to be significantly less soluble in cyclooctane than hydrocarbon-grafted adducts, a shift toward monomer oligomerization can be a potent means of generating a dispersed adduct phase.

Two reactions conducted with a 56:1 C_8H_{16}:TAM ratio reveal the influence of monomer loading (Expts B, C; Table 5.2). These solutions were initially clear when heated to 170°C, but became hazy within the first half-life of the peroxide. Solids became visible shortly thereafter, and a considerable volume of precipitate was observed on reaction vessel surfaces after complete initiator decomposition. Cooling to room temperature led to further phase separation, as TAM-derived products became insoluble in the predominately hydrocarbon medium. Taking the mixture up in xylenes fractionated the mixture into soluble adducts and crosslinked solids, the yields and composition of which are listed in Table 5.2.

Irrespective of peroxide loading, 56:1 C_8H_{16}:TAM reactions carried out at 170°C gave high yields of xylene-soluble compounds whose composition did not differ significantly from those generated from more dilute solutions. The crosslinked precipitate phase was relatively lean in hydrocarbon, with elemental analysis revealing on the order of 0.5 mol of C_8H_{16} per mol TAM. This composition suggests that oligomerization contributes significantly to reaction-induced phase separation, with TAM+C_8H_{16} adducts engaging TAM to produce insoluble material.

Powder x-ray diffraction analysis of the crosslinked solids gave a broad halo that is characteristic of amorphous solids, while differential scanning calorimetry showed no evidence of a significant phase transition from -25°C to 200°C. Figure 5.2a, b contains scanning electron microscopy (SEM) images for solids prepared in Expt. C,

Table 5.2. These images reveal primary particles with sizes on the order of 1-2 μm in various states of aggregation, with a relatively small population of single spheres. Once formed, aggregates could not be affected by pressing the product at 200°C or by sonicating the material in organic solvents.

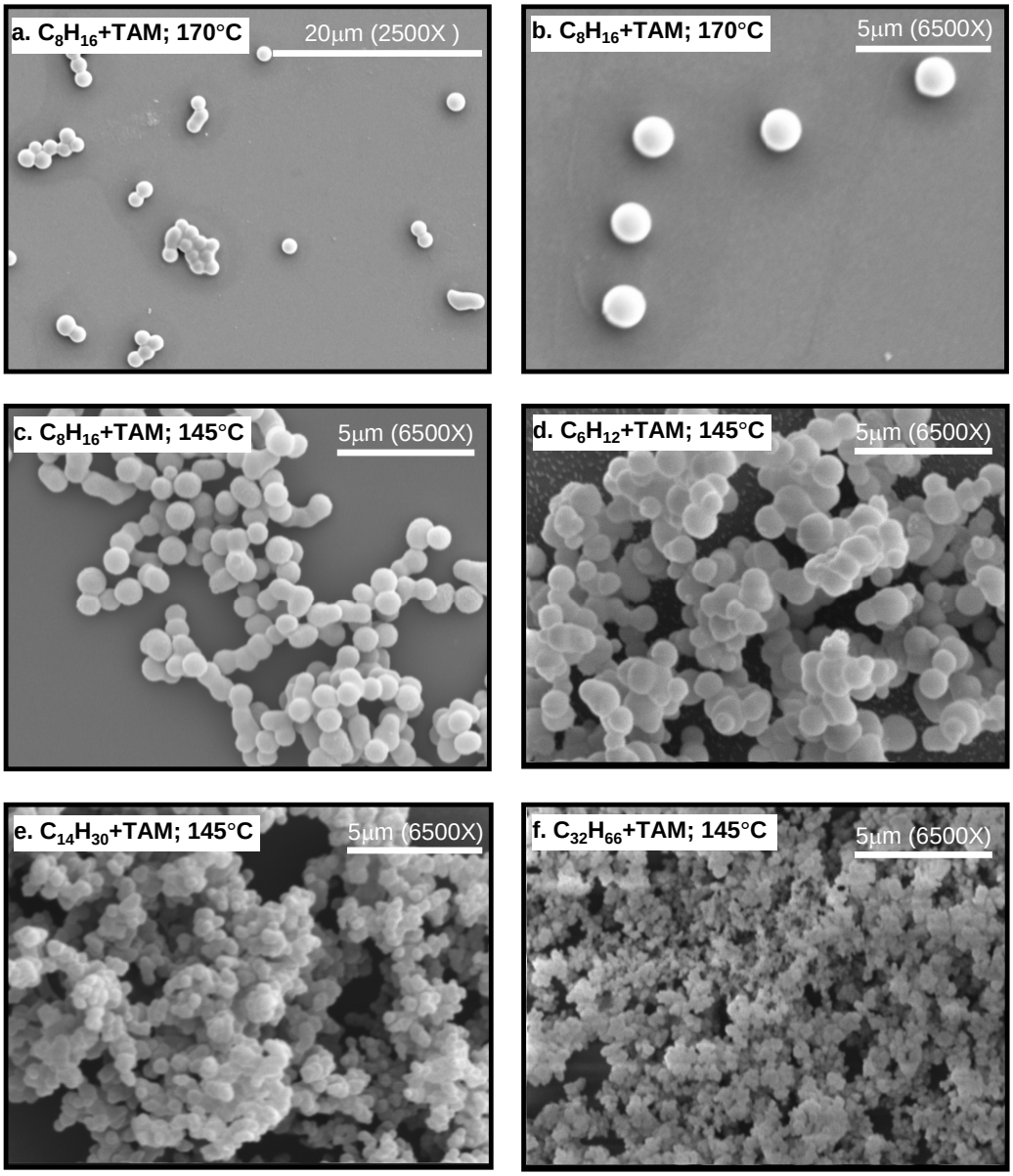

Figure 5. 3 SEM images of isolated solids a,b. Expt C. Table 5.2; c. Expt E, Table 5.2; d. Expt E, Table 5.2 from autoclave; e. Expt B, Table 5.3; f. Expt C, Table 5.3; g. Expt D, Table 5.3.

Coalescence is commonplace for precipitation polymerizations, and its incidence in our process could not be avoided by increasing the intensity of agitation in a stirred autoclave. A hydrocarbon medium is not amenable to ionic surfactants, leaving the steric stabilization methods employed in dispersion polymerizations as the only potential technique for avoiding particle agglomeration. [24] Repeated trials using a block copolymer of ethylene and ethylene oxide did not provide satisfactory results, and further work is needed to produce single, hydrocarbon-rich particles in high yield.

Temperature is a third variable that can be used to affect reaction-induced phase instability by altering the dynamics of radical reactions, the timescales available for phase-partitioning, and the solubility of C_8H_{16}+TAM adducts. Based on available data, it appears that the last factor is the most important. For example, reactions of 56:1 C_8H_{16}:TAM solutions at 145°C converted 18% to 23% of TAM to crosslinked solids, depending on peroxide loading (Expts D-F; Table 5.2). Furthermore, these precipitates contained 0.8 mol C_8H_{16} per mol TAM, as opposed to the 0.5:1.0 maximum generated at 170°C. The higher hydrocarbon content of the precipitated solids, and the depletion of xylene-soluble material, is consistent with a lower solubility of TAM adducts/oligomers .

Based on the SEM image of solids produced at 145°C (Figure 2c; Table 5.2, Expt E), temperature had a marginal effect on the size of cyclooctane-derived particles. Solids generated under these conditions were comprised of primary particles with

sizes on the order of 1-2 μm – comparable to those generated at 170°C. However, aggregation was extensive at this higher solids yield and single particles could not be found amongst reaction products.

Since C-H bond addition to TAM is intended to generate adducts that comprise crosslinked particles, the molar mass of the hydrocarbon will affect overall mass-based reaction yields and the solid phase's crosslink density. Table 5.3 summarizes particle formation experiments with a range of hydrocarbons. Three key differences were observed upon shifting from cyclooctane to other hydrocarbons. The overall particle yield increased, the amount of TAM converted to crosslinked solids increased, as did the molar ratio of monomer to hydrocarbon within the solid fraction.

Table 5. 3: Hydrocarbon + TAM Crosslinked Product Yields [a]

Expt.	Hydrocarbon	Overall Yield[b] wt%	TAM Yield[c] %	RH : TAM Molar Ratio
A	Cyclooctane	1.2	19	0.8:1
B	Cyclohexane	2.9	54	0.3:1
C	Tetradecane	3.2	55	0.3:1
D	Dotriacontane	4.1	66	0.2:1

a. 37 μmole/g DCP; 0.15 mmole TAM/g solution; 145°C
b. Weight percent of total RH + TAM mixture recovered as insoluble solids.
c. Mole percent of TAM recovered in insoluble solids.

These differences can be attributed to the unique grafting reactivity of cyclooctane relative to other hydrocarbons. As noted above, the homolytic C-H bond dissociation energy of cyclooctane is considerably less than that found in other

hydrocarbons (i.e. 389.6 kJ/mol for C_8H_{15}-H versus 400.2 kJ/mol for C_6H_{11}-H), [25] which makes it more susceptible to radical oxidation, and heightens its rate of hydrogen atom donation to alkoxyl and alkyl radicals. Given the importance of hydrogen transfer to graft initiation and propagation, cyclooctane affords higher R-H addition yields and simpler grafting products than other hydrocarbons. [26] In the present context, the lower reactivity of cyclohexane, tetradecane and Dotriacontane resulted in particles that were leaner in hydrocarbon than the corresponding cyclooctane-derived materials.

It is somewhat paradoxical that less reactive hydrocarbons generate higher particle yields. Nevertheless, the data listed in Table 5.3 clearly show that the total amount of particles produced, and the amount of TAM within these particles, was greater for the three alternate hydrocarbons. It is likely that R-H addition to TAM opposes particle formation by consuming the monomer's C=C bonds, and improving the solubility of adducts in the hydrocarbon solution. Therefore, the high grafting reactivity of cyclooctane, while helping to introduce hydrocarbon content to the particles, may hinder the oligomerization and phase-separation processes that give crosslinked particles.

This study concluded with a brief examination of solids morphology generated from different hydrocarbon solutions. The SEM images provided in Figures 2d, e, f reveal a progressive decline in primary particle size on moving from cyclohexane to

tetradecane and further to Dotriacontane. The latter produced coalesced solids with primary particles on the nanometer scale. Our present state of knowledge does not allow us to explain these effects definitively. However, it is likely that the solubility of TAM-derived adducts varies amongst these hydrocarbons, leading to different phase-partitioning behaviour.

5.4 Conclusions.

A new approach to precipitation polymerization has been demonstrated wherein C-H bond addition to a triallyl monomer contributes significantly to the composition of crosslinked solids. This variation may widen the scope of particle syntheses by incorporating non-polymerizable, functional molecules. Advances in steric stabilization are required to limit the extent of microsphere coalescence.

5.5 References.

1. Parent, J.S.; Sengupta, S.S.; Kaufman, M. and Chaudhary, B.I., *Polymer,* **2008**, *49*, 3884-3891.
2. Bamford, C. H.; Ledwith, A. and Sengupta, P. K., *J. Appl. Polym. Sci.*, **1980**, *25*, 2559-2566.
3. Li, K. and Stöver, D. H., *J. Polym. Sci. Part A: Polym. Chem.*, **1993**, *31*, 2473-2479.
4. Song, J. S. and Winnik, M. A., *Macromolecules*, **2005**, *38*, 8300-8307.

5. Barrett, E. J. and Thomas, H. R. In *Dispersion Polymerization in Organic Media*, Barrett, K. E. J., Ed.; Wiley, London, **1975**, pp 115-200.
6. Mackova, H. and Horak, D., *J. Polym. Sci. Part A: Polym. Chem.*, **2005**, *44*, 968-982.
7. Dai, Z.; Yang, X. and Huang, W., *Polym. Int.*, **2007**, *56*, 224-230.
8. Downey, J. S.; Frank, R. S.; Li, W. H. and Stöver, H. D. H. *Macromolecules*, **1999**, *32*, 2838-2844.
9. Li, W. H. and Stöver, H. D. H., *Macromolecules*, **2000**, *33*, 4354-4360.
10. Choi, H. H. and Choe, S., *J. Polym. Sci. Part A: Polym. Chem.*, **2004**, *42*, 835-845.
11. Jin, J. M.; Yang, S.; Sim, S. E. and Choe, S., *J. Polym. Sci. Part A: Polym. Chem.*, **2005**, *43*, 5343-5346.
12. Jin, J. M.; Lee, J. M.; Ha, M. H.; Lee, K. and Choe, S., *Polymer*, **2007**, *48*, 3107-3115.
13. Perrier-Cornet, R.; Heroguez, V.; Thienpont, A.; Babot, O. and Toupance, T., *J. Chromatog. A*, **2008**, *1179*, 2-8.
14. Giese, B., In: *Radicals in Organic Synthesis: Formation of Carbon-Carbon Bonds*, Pergamon Press **1986**.
15. Russell, K. E., *Prog. Polym. Sci.*, **2002**, *27*, 1007-1038.
16. Moad, G., *Prog. Polym. Sci.*, **1999**, *24*, 81-142.
17. Muenger, K. and Fischer, H., *Int. J. Chem. Kin.*, **1985**, *17*, 809-829.
18. Zytowski, T. and Fischer, H., *J. Amer. Chem. Soc.*, **1996**, *118*, 437-439.

19. Sengupta, S. S.; Parent, J. S.; McLean, J. K., *J. Polym. Sci. Part A: Polym. Chem.*, **2005**, *43*, 4882-4883.

20. Fitch, R. M., *J. Elastoplastics*, **1971**, *3*, 146-156.

21. Bartlett, P. D. and Altschul, R., *J. Amer. Chem. Soc.*, **1945**, *67*, 816-822.

22. Bartlett, P. D. and Tate, F. A., *J. Amer. Chem. Soc.*, **1953**, *75*, 91-95.

23. Litt, M. and Eirich, F. R., *J. Polym. Sci.*, **1960**, *45*, 379-396.

24. Waldbridge, D. J., In: *Dispersion Polymerization in Organic Media*, Barrett, K. E. J., Ed.; Wiley, London, **1975**; pp 45-114.

25. Fujisaki, N.; Ruf, A. and Gaumann T., *J. Amer. Chem. Soc.*, **1985**, *107*, 1605-1610.

26. Wu, W. and Parent, J. S., J. Polym. Sci. Part A : Polym. Chem., **2008**, *46*, 7386-7394.

Chapter 6: Summary Comments and Recommendations for Further Research

This thesis project has examined conventional peroxide-initiated vinylsilane and allyl monomer grafting to saturated hydrocarbons, high-temperature bicumene-initiated extensions of this chemistry, and unconventional alkyne addition reactions, all with the intent of generating functional derivatives of relatively stable, non-polar polymers and small molecules.

A common thread weaves through the discussions of each chapter – hydrogen atom transfer. Irrespective of the type of initiator, monomer, or hydrocarbon, hydrogen atom transfer rates have been shown to dominate the dynamics and yields of modification processes. In the case of conventional silane grafting kinetics (Chapter 2), the high activation energy for hydrogen atom abstraction by intermediate monomer-derived radicals was implicated as a factor in the insensitivity of grafting yields to temperature. In the case of bicumene-mediated grafting (Chapter 3), hydrogen atom abstraction by cumyl radicals from the hydrocarbon was shown to be an important initiation pathway under oxygen-limited conditions. Although this particular hydrogen atom transfer is relatively unfavourable, the process supports a macro-radical population that is sufficient to sustain an efficient, high-temperature grafting process.

Free radical additions of saturated polymers to alkynes proved to be extremely sensitive to the rate of vinyl radical quenching by the hydrocarbon (Chapter 4).

Where good hydrogen donors such as cyclooctane and poly(ethylene oxide) were used, a high yield of simple di-substituted acrylates were observed. However, sluggish hydrogen atom donation to intermediate vinyl radicals led to a predominance of oligomeric products and tri-substituted aromatic compounds, and lower overall alkyne conversions.

The influence of hydrogen transfer on particle formation is quite complicated (Chapter 5). Whereas simple grafting of cyclooctane to TAM is needed to produce particles that contain the hydrocarbon, it is the precipitation of TAM-derived oligomers that supports particle formation. The balance between hydrocarbon addition to TAM (which improves monomer solubility) and repeated TAM addition (which results in phase instability) is dictated by the relative rates of monomer-derived radical trapping by hydrogen abstraction relative to repeated C=C addition. As such, hydrocarbon-rich particle formation is contingent on the relative efficiency of these two radical reactions.

Given the importance of hydrogen atom transfer to radical-mediated polymer modification, deliberate studies of these reactions are recommended for further research. Experimental measurements of hydrogen transfer rates must be made at the high temperatures that are relevant to semi-crystalline polymer modification, in contrast to existing reports that focus on near ambient temperatures. Preliminary efforts to quantify the hydrogen atom donor qualities of different polymers have been

undertaken by the Parent group that involve simple measurements of cumyloxyl radical byproducts. Further investment in this line of research should provide tangible benefits in terms of understanding polyolefin modification chemistry.